Mathematical Biosciences and Engineering

http://www.aimspress.com/journal/mbe

MBE, 20(11): 19372–19400.
DOI: 10.3934/mbe.2023857
Received: 24 May 2023
Revised: 20 September 2023
Accepted: 06 October 2023
Published: 18 October 2023

Research article

Spatiotemporal dynamics of a diffusive predator-prey model with delay and Allee effect in predator

Fang Liu and Yanfei Du*

School of Mathematics and Data Science, Shaanxi University of Science and Technology, Xi'an 710021, China

* **Correspondence:** Email:duyanfei@sust.edu.cn.

Abstract: It has been shown that Allee effect can change predator-prey dynamics and impact species persistence. Allee effect in the prey population has been widely investigated. However, the study on the Allee effect in the predator population is rare. In this paper, we investigate the spatiotemporal dynamics of a diffusive predator-prey model with digestion delay and Allee effect in the predator population. The conditions of stability and instability induced by diffusion for the positive equilibrium are obtained. The effect of delay on the dynamics of system has three different cases: (a) the delay doesn't change the stability of the positive equilibrium, (b) destabilizes and stabilizes the positive equilibrium and induces stability switches, or (c) destabilizes the positive equilibrium and induces Hopf bifurcation, which is revealed (numerically) to be corresponding to high, intermediate or low level of Allee effect, respectively. To figure out the joint effect of delay and diffusion, we carry out Turing-Hopf bifurcation analysis and derive its normal form, from which we can obtain the classification of dynamics near Turing-Hopf bifurcation point. Complex spatiotemporal dynamical behaviors are found, including the coexistence of two stable spatially homogeneous or inhomogeneous periodic solutions and two stable spatially inhomogeneous quasi-periodic solutions. It deepens our understanding of the effects of Allee effect in the predator population and presents new phenomena induced be delay with spatial diffusion.

Keywords: Allee effect in predator; digestion delay; stability switches; Turing-Hopf bifurcation; normal form

1. Introduction

Since the pioneering work of Lotka [1] and Volterra [2], predator-prey models have been studied in depth by many biologists and mathematicians. Numerous studies have shown that Allee effect will greatly promote the extinction of the population. Most of the present studies focus on the Allee effect on prey populations [3–5]. In fact, Allee effect can also occur in predators due to a great variety of

mechanisms such as cooperative breeding, mating difficulty and sperm limitation [6]. Among them, mating difficulty mechanism occurs widely across a variety of predatory species, from invertebrates to vertebrates [7–9], which is a reduced probability of finding mates at low densities.

Zhou et al. [3] considered Lotka-Volterra and Leslie-type predator-prey models with Allee effect in predators, and found that Allee effect may be a destabilizing factor in predator-prey models. Sen et al. [10] explored a predator-prey model with Allee effect in predators which affects the numerical response of predators without affecting its functional response

$$\begin{cases} \frac{\mathrm{d}N}{\mathrm{d}T} = rN\left(1-\frac{N}{K}\right) - \frac{aNP}{1+aqN}, \\ \frac{\mathrm{d}P}{\mathrm{d}T} = e\psi(P)\frac{aNP}{1+aqN} - \mu P, \end{cases} \tag{1.1}$$

where N and P represent the population densities of the prey and predators respectively, r is the intrinsic growth rate of the prey and K is the carrying capacity, a is the encounter rate of the prey and predators, q describes the handling time, $e\psi(P)$ is food conversion efficiency of predators, $\psi(P)$ models the Allee effect in predator and μ is the intrinsic death rate of predators. The bifurcation structure of the model including saddle-node, Hopf, generalized Hopf and Bogdanov-Takens bifurcation have been investigated. To describe the Allee effect in predators, different expressions for $\psi(P)$ are used, such as $\frac{P}{B+P}$ [3, 10–12], $\tan h\left(\frac{P}{B}\right)$ [10], $r(P-B)\left(1-\frac{P}{K}\right)$ [13], $1-e^{-PB}$ [14] and $e^{-\frac{P}{B}}$ [15], where B represents the strength of Allee effect.

Predators and prey tend to move from high-density areas to low-density areas in response to resource distribution, invasion of natural enemies, human exploitation and natural disasters. Therefore, adding the diffusion term to the predator-prey model will make the model more reasonable. Time delays are ubiquitous in the process of predator and prey interaction. After predators consume the prey, the reproduction of predators is not instantaneous. Rather, it takes a certain amount of time to convert the prey energy into their own energy, which is known as digestion delay. There is an extensive literature on predator-prey models with digestion delay [16–18]. It shows that the digestion delay has very complex effect on the dynamics of a system. For example, it can destabilize the equilibrium and induce periodic oscillations. Thus, the digestion delay cannot be ignored and should be introduced into the predator-prey model.

Inspired by Sen et al. [10] and the previous work, we choose $\frac{P}{B+P}$ [3, 12] as the mating difficulty induced Allee effect term, where B is the Allee effect constant and $\frac{P}{B+P}$ describes the probability that a female finds and mates with a least one male. Introducing diffusion and digestion delay into model (1.1), one can obtain the following model

$$\begin{cases} \frac{\partial N}{\partial T} = D_1\Delta N_{xx} + rN\left(1-\frac{N}{K}\right) - \frac{aNP}{1+aqN}, & x\in\Omega, T>0, \\ \frac{\partial P}{\partial T} = D_2\Delta P_{xx} + \frac{eP}{B+P}\cdot\frac{aN(x,T-\tau)P(x,T-\tau)}{1+aqN(x,T-\tau)} - \mu P, & x\in\Omega, T>0, \\ \frac{\partial N(x,T)}{\partial x} = \frac{\partial P(x,T)}{\partial x} = 0, & x\in\partial\Omega, T>0, \\ N(x,T) = N_0(x,T)\geq 0, P(x,T) = P_0(x,T)\geq 0, & x\in\overline{\Omega}, T\in[-\tau,0], \end{cases} \tag{1.2}$$

where τ is the digestion delay and D_1 and D_2 are diffusion coefficients characterizing the rate of the spatial dispersion of the prey and predator population, respectively. The homogeneous Neumann boundary conditions means that predators and the prey live in a self-contained environment (e.g., an island, lake, pond, etc.) and there is no population flux on the boundary. In reality, there may be a scenario that the boundary is hostile and no individuals would choose to leave. In this case, the

homogeneous Dirichlet boundary conditions should be proposed on the boundary, and there is no positive constant steady state. In this paper, we are interested in the bifurcations from the positive constant steady state, corresponding to the homogeneous Neumann boundary condition. We consider the spatial domain $\Omega = (0, l\pi)$. In fact, one-dimensional space can be used for some biological scenarios, such as a long river or depth of the water, etc. For general interval (a, b), we can transform it into $(0, l\pi)$ by a translation and rescaling. Moreover, we can calculate the eigenfunctions of the Laplacian and compute normal forms. The meanings of other parameters in this model are consistent with those expressed in model (1.1). Since the spatial distributions of predators and the prey are different and they may have different moving ability and life habits, the diffusion coefficients D_1 and D_2 are considered different. For the sake of simplicity, set

$$u = \frac{N}{K}, \quad v = \frac{P}{Krq}, \quad t = rT.$$

Model (1.2) is converted into

$$\begin{cases} \frac{\partial u}{\partial t} = d_1 u_{xx} + u(1-u) - \frac{uv}{\beta+u}, & x \in (0, l\pi), t > 0, \\ \frac{\partial v}{\partial t} = d_2 v_{xx} + \frac{\alpha u(x,t-\tau)v(x,t-\tau)}{\beta+u(x,t-\tau)} \cdot \frac{v}{\delta+v} - mv, & x \in (0, l\pi), t > 0, \\ \frac{\partial u(x,t)}{\partial x} = \frac{\partial v(x,t)}{\partial x} = 0, & x = 0, l\pi, t > 0, \\ u(x,t) = u_0(x,t) \geq 0, v(x,t) = v_0(x,t) \geq 0, & x \in [0, l\pi], t \in [-\tau, 0], \end{cases} \tag{1.3}$$

where the new parameters are

$$\alpha = \frac{e}{qr}, \quad \beta = \frac{1}{aqK}, \quad \delta = \frac{B}{Kqr}, \quad m = \frac{\mu}{r}, \quad d_1 = \frac{D_1}{r}, \quad d_2 = \frac{D_2}{r}.$$

To figure out how Allee effect affects the dynamics of system, there has been an extensive literature investigating the dynamics of predator-prey model with Allee effect from the point of bifurcation analysis [19–24]. Wang et al. [25] considered a diffusive Holling-Tanner predator-prey model in which the predator population is subjected to Allee effect and investigated the stability of positive equilibrium and Turing instability. Numerical simulations revealed that the system exhibits a variety of Turing patterns, such as holes, stripes and spots. Tyutyunov et al. [26] studied a prey-taxis model based on nonspatial Rosenzweig-MacArthur model and found that formation of local dense aggregations caused by prey-taxis will allow predators to overcome the Allee effect in its population growth, avoiding the extinction that occurs in the model in the absence of spatial effects. Rana et al. [27] examined a diffusive Leslie-Gower predator-prey model with Allee effect in both predator and prey populations. They obtained the conditions for Hopf bifurcation, Turing bifurcation and explored complex dynamical phenomena of the system.

Although there has some literature on predator-prey model with Allee effect on predator and diffusion, no work has been done to reveal the joint impact of Allee effect, diffusion and digestion delay on the population dynamics. Our goal in this paper is to investigate the complex spatiotemporal patterns induced by delay and diffusion in predator-prey model with Allee effect in predators. For the non delayed system, we obtain the conditions for the stability and instability induced by diffusion for the positive equilibrium $E_3(u_3, v_3)$. For the delayed system, we find that there are three different cases of the occurrence of Hopf bifurcation. Combining with numerical simulations, we find that when the

strength of Allee effect δ is low, delay τ will destabilize $E_3(u_3, v_3)$ and induce Hopf bifurcation; when δ is at an intermediate value, delay τ will induce Hopf bifurcation and stability switches and when δ is high, Hopf bifurcation will not occur. To reveal the spatiotemporal dynamics, Turing-Hopf bifurcation analysis is carried out, from which the clarification of dynamics near Turing-Hopf bifurcation point is obtained, including the existence of spatially homogeneous and inhomogeneous periodic solutions and spatially inhomogeneous quasi-periodic solutions.

The present paper is organized as follows. In Section 2, we first give the existence and local stability of positive equilibria. Then, we derive the conditions for Turing instability, Hopf bifurcation and Turing-Hopf bifurcation. In Section 3, the normal form of Turing-Hopf bifurcation is derived. Some numerical simulations are carried out to illustrate our theoretical results in Section 4. Finally, a summary of our findings is presented in Section 5.

2. Stability of positive equilibria and bifurcation analysis

In this section, we will study the existence of Turing, Hopf and Turing-Hopf bifurcation by linear stability analysis.

2.1. Existence of equilibria

First, we consider the existence of equilibria for system (1.3). In this subsection, we focus on the spatially homogeneous model (1.1), which is a model of ordinary differential equations corresponding to the system (1.3). Obviously, system (1.3) always has a trivial equilibrium $E_1(0, 0)$ and a predator-free equilibrium $E_2(1, 0)$. The coexistence equilibrium will be the intersection of the following two non trivial nullclines in the interior of the first quadrant

$$\begin{cases} f(u, v) \equiv 1 - u - \frac{v}{\beta+u} = 0, \\ g(u, v) \equiv \frac{\alpha u v}{(\beta+u)(\delta+v)} - m = 0, \end{cases} \tag{2.1}$$

which can be written as

$$v_1(u) = (1 - u)(\beta + u), \quad v_2(u) = \frac{(\beta + u)\delta m}{\alpha u - (\beta + u)m}. \tag{2.2}$$

The biological feasibility of v_i yields that $\frac{\beta m}{\alpha - m} < u_i < 1$ with $\alpha > m$. Solving $v_1(u) = v_2(u)$ leads to

$$A_1 u^2 + A_2 u + A_3 = 0, \tag{2.3}$$

where

$$A_1 = \alpha - m, \quad A_2 = m(1 - \beta) - \alpha, \quad A_3 = m(\beta + \delta).$$

The number of interior equilibria is consistent with that of positive roots of Eq (2.3), which depends on the signs of $\Delta = A_2^2 - 4A_1A_3$ and A_2. A direct calculation yields that when $\Delta = 0$, we have $\delta = \frac{[\alpha-(1+\beta)m]^2}{4m(\alpha-m)}$. Therefore, one can get the existence of equilibria for system (1.3).

Theorem 2.1. *Suppose that $\alpha > m$.*

(i) If $0 < \delta < \frac{[\alpha-(1+\beta)m]^2}{4m(\alpha-m)}$ *and* $m(1-\beta) < \alpha$, *system* (1.3) *has two equilibria* $E_3(u_3, v_3)$ *and* $E_4(u_4, v_4)$, *where*

$$\begin{aligned} u_3 &= \frac{-A_2 - \sqrt{A_2^2 - 4A_1A_3}}{2A_1}, \quad v_3 = \frac{(\beta+u_3)\delta m}{\alpha u_3 - (\beta+u_3)m}, \\ u_4 &= \frac{-A_2 + \sqrt{A_2^2 - 4A_1A_3}}{2A_1}, \quad v_4 = \frac{(\beta+u_4)\delta m}{\alpha u_4 - (\beta+u_4)m}. \end{aligned} \tag{2.4}$$

(ii) If $\delta = \frac{[\alpha-(1+\beta)m]^2}{4m(\alpha-m)}$ *and* $m(1-\beta) < \alpha$, *system* (1.3) *has a unique positive equilibrium* $E_5(u_5, v_5)$, *where*

$$u_5 = -\frac{A_2}{2A_1}, \quad v_5 = \frac{(\beta+u_5)\delta m}{\alpha u_5 - (\beta+u_5)m}.$$

(iii) If $\delta > \frac{[\alpha-(1+\beta)m]^2}{4m(\alpha-m)}$, *system* (1.3) *has no positive equilibria.*

Remark 2.2. *From Theorem 2.1, we obtain that system* (1.3) *may have no, one or two equilibria with different values of the strength of Allee effect* δ *(see Figure 1(a)). Figure 1(b) gives the relationship between* u_i (v_i) *and* δ. *When* $\delta \le \delta^* = 0.1383$, *predators and the prey can coexist. However, when* $\delta > 0.1383$, *predators and the prey cannot coexist. If* $\delta < 0.1383$, u_3 (v_3) *is increasing (decreasing) when* δ *increases and* u_4 (v_4) *is decreasing (increasing) when* δ *increases.*

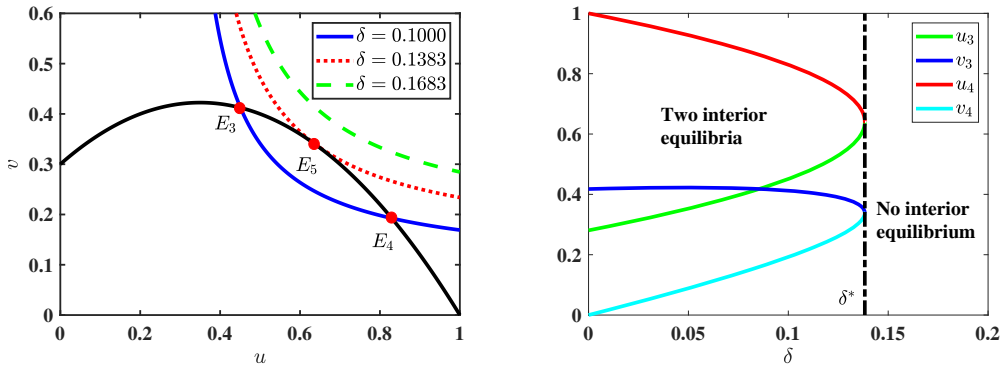

(a) **(b)**

Figure 1. (a) The black curve is the figure of $f(u, v) = 0$, where $f(u, v)$ is defined in (2.1). The blue, red and green curves are the figures for $g(u, v)$=0 for $\delta = 0.1000$, $\delta = 0.1383$, and $\delta = 0.1683$, respectively. (b) The curves of u_i and v_i $(i = 3, 4)$ with varying δ. Other parameters are $\alpha = 1.2, \beta = 0.3$ and $m = 0.58$.

2.2. Turing instability for the non delayed system

In this subsection, we consider the stability and diffusion-driven instability of the positive equilibria $E_i(u_i, v_i)$ $(i = 3, 4)$ when $\tau = 0$, i.e., the non delayed system corresponding to system (1.3)

$$\begin{cases} \frac{\partial u}{\partial t} = d_1 u_{xx} + u(1-u) - \frac{uv}{\beta+u}, & x \in (0, l\pi), t > 0, \\ \frac{\partial v}{\partial t} = d_2 v_{xx} + \frac{\alpha u v^2}{(\beta+u)(\delta+v)} - mv, & x \in (0, l\pi), t > 0, \\ \frac{\partial u(x,t)}{\partial x} = \frac{\partial v(x,t)}{\partial x} = 0, & x = 0, l\pi, t > 0, \\ u(x,0) = u_0(x) \geq 0, v(x,0) = v_0(x) \geq 0, & x \in [0, l\pi]. \end{cases} \tag{2.5}$$

In the rest of this paper, we assume that

$$(H_1)\ \ 0 < \delta < \frac{[\alpha - (1+\beta)m]^2}{4m(\alpha - m)} \text{ and } m(1-\beta) < \alpha$$

holds for the existence of positive equilibria.

The linearization of system (2.5) at the positive equilibria $E_i(u_i, v_i)$ $(i = 3, 4)$ can be expressed by

$$\frac{\partial}{\partial t}\begin{pmatrix} u \\ v \end{pmatrix} = D\begin{pmatrix} \Delta u \\ \Delta v \end{pmatrix} + \begin{pmatrix} a_{11} & a_{12} \\ a_{21} & a_{22} \end{pmatrix}\begin{pmatrix} u \\ v \end{pmatrix}, \tag{2.6}$$

where $D = \mathrm{diag}(d_1, d_2)$ and

$$\begin{aligned} a_{11} =& u f_u(u,v)|_{E_i} = \left.\frac{u(1-\beta-2u)}{\beta+u}\right|_{E_i}, \quad a_{12} = u f_v(u,v)|_{E_i} = -\left.\frac{u}{\beta+u}\right|_{E_i} < 0, \\ a_{21} =& v g_u(u,v)|_{E_i} = \left.\frac{m\beta v}{(\beta+u)u}\right|_{E_i} > 0, \quad a_{22} = v g_v(u,v)|_{E_i} = \left.\frac{m\delta}{\delta+v}\right|_{E_i} > 0, \end{aligned} \tag{2.7}$$

with $i = 3, 4$. It is well known that the eigenvalue problem

$$\Delta\phi(x) = \lambda\phi(x), \quad x \in (0, l\pi), \quad \frac{\partial\phi(0)}{\partial x} = \frac{\partial\phi(l\pi)}{\partial x} = 0$$

has eigenvalues $\lambda_n = -\frac{n^2}{l^2}(n \in \mathbb{N}_0)$, with the corresponding eigenfunctions

$$\beta_n(x) = \frac{\cos\frac{n}{l}x}{\left\|\cos\frac{n}{l}x\right\|_{L^2}} = \begin{cases} \sqrt{\frac{1}{l\pi}}, & n = 0, \\ \sqrt{\frac{2}{l\pi}}\cos\frac{n}{l}x, & n \geq 1. \end{cases}$$

The characteristic equation for the linearized system (2.6) is

$$\lambda^2 + T_n\lambda + D_n = 0,\ n \in \mathbb{N}_0, \tag{2.8}$$

where

$$T_n = (d_1 + d_2)\frac{n^2}{l^2} + T_0, \quad D_n = d_1 d_2 \frac{n^4}{l^4} - (d_1 a_{22} + d_2 a_{11})\frac{n^2}{l^2} + D_0, \tag{2.9}$$

with $T_0 = -(a_{11} + a_{22})$, $D_0 = a_{11}a_{22} - a_{12}a_{21}$.

Lemma 2.3. *Suppose that (H_1) holds. For $E_3(u_3, v_3)$, $D_0 = a_{11}a_{22} - a_{12}a_{21} > 0$ and for $E_4(u_4, v_4)$ $D_0 < 0$.*

Proof. From (2.1) and (2.2), we have

$$f_u(u, v) = -f_v(u, v)\frac{\mathrm{d}v_1(u)}{\mathrm{d}u}, \quad g_u(u, v) = -g_v(u, v)\frac{\mathrm{d}v_2(u)}{\mathrm{d}u}.$$

Thus, D_0 can be written as

$$D_0 = \left[uvf_v(u, v)g_v(u, v)\left(\frac{\mathrm{d}v_2(u)}{\mathrm{d}u} - \frac{\mathrm{d}v_1(u)}{\mathrm{d}u}\right)\right]_{(u_i,v_i)}.$$

From the qualities of nullclines, we can easily get

$$\left(\frac{\mathrm{d}v_2(u)}{\mathrm{d}u} - \frac{\mathrm{d}v_1(u)}{\mathrm{d}u}\right)\Bigg|_{(u_3,v_3)} < 0 \quad \text{and} \quad \left(\frac{\mathrm{d}v_2(u)}{\mathrm{d}u} - \frac{\mathrm{d}v_1(u)}{\mathrm{d}u}\right)\Bigg|_{(u_4,v_4)} > 0.$$

From (2.7), we have $f_v(u, v) < 0$ and $g_v(u, v) > 0$, which lead to $D_0|_{(u_3,v_3)} > 0$ and $D_0|_{(u_4,v_4)} < 0$. □

From Lemma 2.3, we have $D_0|_{E_4} < 0$, which indicates that $E_4(u_4, v_4)$ is unstable. To investigate the stability of $E_3(u_3, v_3)$, denote

$$(H_2)\ u_3 > \frac{1}{2}\left[1 - \beta + \frac{m\delta(\beta + u_3)}{u_3(\delta + v_3)}\right].$$

It is easy to get that if (H_2) holds, $T_0 > 0$. We have $T_n \geq T_0 > 0$, for $n \in \mathbb{N}_0$.

To have diffusion-driven instability, we need to find at least one positive integer n, such that $D_n < 0$. We choose diffusion coefficient d_1 as the bifurcation parameter to analyze the Turing bifurcation. For $E_3(u_3, v_3)$, we easily obtain from $D_n = 0$ that

$$d_1\left(n^2\right) = \frac{\left(a_{11}d_2n^2 - D_0l^2\right)l^2}{n^2\left(d_2n^2 - a_{22}l^2\right)}, \tag{2.10}$$

where a_{11}, a_{22} and D_0 are defined in (2.7) and (2.9).

Denote

$$d_1^* = \min_{n\in\mathbb{N}} d_1(n^2). \tag{2.11}$$

Thus, we have the following results.

Lemma 2.4. *Assume that (H_1) and (H_2) hold. For $E_3(u_3, v_3)$, we have*

(i) If $d_1 < d_1^*$, $D_n > 0$ for all $n \in \mathbb{N}$.

(ii) If $d_1 > d_1^*$, there exist $n \in \mathbb{N}$ such that $D_n < 0$.

Proof. Since (H_2) holds, we have $u_3 > \frac{1-\beta}{2}$. Thus, $a_{11} < 0$ and $(a_{11}d_2n^2 - D_0l^2)l^2 < 0$. Therefore, we can deduce that $d_1(n^2) > 0$ if $n^2 < \frac{a_{22}l^2}{d_2}$. For $n^2 < \frac{a_{22}l^2}{d_2}$, we obtain

$$D_n\begin{cases} > 0, & d_1 < d_1(n^2), \\ = 0, & d_1 = d_1(n^2), \\ < 0, & d_1 > d_1(n^2). \end{cases}$$

Let $q = n^2$. Equation (2.10) can be written as

$$d_1(q) = \frac{\left(a_{11}d_2q - D_0l^2\right)l^2}{q\left(d_2q - a_{22}l^2\right)}. \tag{2.12}$$

Differentiating both sides of Eq (2.12) with respect to q yields

$$d_1'(q) = \frac{l^2\left(-a_{11}d_2^2q^2 + 2D_0d_2l^2q - D_0a_{22}l^4\right)}{q^2\left(d_2q - a_{22}l^2\right)^2}\begin{cases}\leq 0, & 0 < q \leq q^*,\\ > 0, & q > q^*,\end{cases}$$

where

$$q^* = \frac{\left(D_0 - \sqrt{D_0^2 - D_0a_{11}a_{22}}\right)l^2}{a_{11}d_2}.$$

$d_1(q)$ reaches its minimum at $q = q^*$. To sum up, the range of wave numbers for the occurrence for Turing instability is $n^2 < a_{22}l^2/d_2$, and when $d_1 > d_1\left(n^2\right)$, $D_n < 0$. Now, we need to find the critical wave number N_* such that $d_1\left(n^2\right)$ reaches its minimum at $n = N_*$. In fact,

$$N_* = \begin{cases}N_0, & d_1\left(N_0^2\right) \leq d_1\left((N_0+1)^2\right),\\ N_0+1, & d_1\left(N_0^2\right) > d_1\left((N_0+1)^2\right),\end{cases}$$

here $N_0 = \lfloor\sqrt{q^*}\rfloor$, where $\lfloor\cdot\rfloor$ is the floor function. Thus, we have $d_1^* \triangleq d_1\left(N_*^2\right) = \min\limits_{n\in\mathbb{N}} d_1(n^2)$. □

From the above analysis, we get the following conclusion.

Theorem 2.5. *Assume that (H_1) and (H_2) hold and d_1^* is defined in* (2.11)*. For non delayed system* (2.5)*, we have*

(i) If $d_1 < d_1^*$, $E_3(u_3, v_3)$ is locally asymptotically stable.

(ii) If $d_1 > d_1^*$, $E_3(u_3, v_3)$ is unstable.

(iii) System (2.5) *undergoes a Turing bifurcation at $E_3(u_3, v_3)$ when $d_1 = d_1^*$.*

2.3. Hopf and Turing-Hopf bifurcation for the delayed system

In this section, we investigate the effect of delay τ on the dynamics for system (1.3).

For Neumann boundary condition, we define the real-valued Hilbert space

$$X := \left\{(u, v) \in H^2(0, l\pi) \times H^2(0, l\pi) \,\middle|\, \frac{\partial u(x,t)}{\partial x} = \frac{\partial v(x,t)}{\partial x} = 0 \text{ at } x = 0, l\pi\right\}$$

and the corresponding complexification space $X_{\mathbb{C}} := X \oplus \mathrm{i}X = \{U_1 + \mathrm{i}U_2 | U_1, U_2 \in X\}$ with the general complex-value L^2 inner product $\langle U_1, U_2\rangle = \int_0^{l\pi}(\bar{u}_1u_2 + \bar{v}_1v_2)\mathrm{d}x$, where $U_i = (u_i, v_i)^T \in X_{\mathbb{C}}$, $i = 1, 2$. Let $C_\tau := C([-\tau, 0], X_{\mathbb{C}})$ denote the phase space with the sup norm $|\phi| = \sup\limits_{-\tau\leq\theta\leq 0}|\phi(\theta)|$. The linearization system of (1.3) at $E_3(u_3, v_3)$ can be rewritten in the space C_τ as

$$\frac{\mathrm{d}U(t)}{\mathrm{d}t} = D\Delta U(t) + L\left(U^t\right), \tag{2.13}$$

where $D = \text{diag}(d_1, d_2)$, $U(t) = (u(x,t), v(x,t))^T$, $U^t \in C_\tau$ and $L(\cdot) : C_\tau \to X_{\mathbb{C}}$ is a bounded linear operator defined by

$$L(\phi) = L_1\phi(0) + L_2\phi(-\tau),$$

where

$$L_1 = \begin{pmatrix} a_{11} & a_{12} \\ 0 & \widetilde{a}_{22} \end{pmatrix}, \quad L_2 = \begin{pmatrix} 0 & 0 \\ b_{21} & m \end{pmatrix}, \tag{2.14}$$

with a_{11}, a_{12} are defined in (2.7) and

$$\widetilde{a}_{22} = -\frac{mv_3}{\delta + v_3} < 0, \quad b_{21} = \frac{m\beta v_3}{(\beta + u_3)u_3} > 0.$$

The characteristic equation of (2.13) is

$$\lambda^2 + A_n\lambda + B_n + (C_n - m\lambda)e^{-\lambda\tau} = 0, \ n \in \mathbb{N}_0, \tag{2.15}$$

where

$$\begin{aligned} A_n =& (d_1 + d_2)\frac{n^2}{l^2} - a_{11} - \widetilde{a}_{22}, \\ B_n =& d_1 d_2 \frac{n^4}{l^4} - (d_1\widetilde{a}_{22} + d_2 a_{11})\frac{n^2}{l^2} + a_{11}\widetilde{a}_{22}, \\ C_n =& - a_{12}b_{21} - m\left(\frac{n^2}{l^2}d_1 - a_{11}\right). \end{aligned}$$

When $\tau = 0$, Eq (2.15) can be written as (2.8), where $T_n = A_n - m$, $D_n = B_n + C_n$. To investigate the effect of delay τ, we assume that $E_3(u_3, v_3)$ is stable for non delayed system. From the previous section, we assume that (H_1), (H_2) and $d_1 < d_1^*$ hold for the stability of $E_3(u_3, v_3)$ when $\tau = 0$.

If $\pm i\omega_0$ ($\omega_0 > 0$) is a pair of roots of (2.15), then we have

$$-\omega_0^2 + i\omega_0 A_n + B_n + (-i\omega_0 m + C_n)\left[\cos(\omega_0\tau) - i\sin(\omega_0\tau)\right] = 0. \tag{2.16}$$

Separating the real and imaginary parts of (2.16), we have

$$\begin{cases} \omega_0^2 - B_n = C_n\cos(\omega_0\tau) - m\omega_0\sin(\omega_0\tau), \\ \omega_0 A_n = C_n\sin(\omega_0\tau) + m\omega_0\cos(\omega_0\tau). \end{cases} \tag{2.17}$$

which is equivalent to

$$\begin{cases} \sin(\omega_0\tau) = \frac{\omega_0(A_nC_n + mB_n - m\omega_0^2)}{m^2\omega_0^2 + C_n^2} \triangleq \mathcal{S}_n(\omega_0), \\ \cos(\omega_0\tau) = \frac{C_n\omega_0^2 + mA_n\omega_0^2 - B_nC_n}{m^2\omega_0^2 + C_n^2} \triangleq C_n(\omega_0). \end{cases} \tag{2.18}$$

Squaring and adding both sides of (2.17) gives us

$$\omega_0^4 + P_n\omega_0^2 + Q_n = 0, \tag{2.19}$$

where

$$P_n = A_n^2 - 2B_n - m^2, \quad Q_n = B_n^2 - C_n^2.$$

Denote $R_n = P_n^2 - 4Q_n$ and $s_n = \omega_0^2$, we can write (2.19) as

$$G(s) \equiv s_n^2 + P_n s_n + Q_n = 0. \tag{2.20}$$

Obviously, the existence of purely imaginary roots of (2.15) depends on the existence of positive roots of (2.20). Since the number of positive roots of (2.20) may be zero, one or two. In the following, we discuss in three cases and make the following assumptions.

(H_3) (i) $R_n < 0$ or (ii) $R_n \geq 0$, $P_n > 0$ and $B_n - C_n > 0$.

(H_4) $B_n - C_n < 0$.

(H_5) $R_n > 0$, $P_n < 0$ and $B_n - C_n > 0$.

If (H_3) holds, Eq (2.20) has no positive roots, which indicates that Eq (2.15) has no purely imaginary roots. Therefore, $E_3(u_3, v_3)$ is always locally asymptotically stable for all $\tau > 0$.

If (H_4) holds, Eq (2.20) has a unique positive root

$$s_n^+ = \frac{1}{2}(-P_n + \sqrt{R_n}).$$

Correspondingly, Eq (2.15) has a pair of purely imaginary roots $\pm \mathrm{i}\omega_n = \pm \mathrm{i}\sqrt{s_n^+}$. From (2.18), we have

$$\tau_{n,j} = \begin{cases} \frac{1}{\omega_n} \arccos C_n(\omega_n) + \frac{2j\pi}{\omega_n}, & \mathcal{S}_n(\omega_n) > 0, \\ -\frac{1}{\omega_n} \arccos C_n(\omega_n) + \frac{2(j+1)\pi}{\omega_n}, & \mathcal{S}_n(\omega_n) < 0, \end{cases} \tag{2.21}$$

for $n \in \mathbb{N}_0$, $j \in \mathbb{N}_0$. Now, we verify the transversality conditions. Differentiating (2.15) with respect to τ, we obtain

$$\operatorname{sign}\left\{\frac{\mathrm{d}(\mathrm{Re}\lambda)}{\mathrm{d}\tau}\right\}\Big|_{\lambda=\mathrm{i}\omega_n} = \operatorname{sign}\left\{\frac{2\omega_n^2 + P_n}{m^2\omega_n^2 + C_n^2}\right\} = \operatorname{sign}\left\{\frac{\sqrt{R_n}}{m^2\omega_n^2 + C_n^2}\right\} > 0.$$

Denote

$$\mathfrak{S}_1 = \{n \in \mathbb{N}_0 |\ (H_4) \text{ holds}\}.$$

For any $n \in \mathfrak{S}_1$, define $\tau_* = \min\limits_{n\in\mathfrak{S}_1}\{\tau_{n,0}\}$ as the smallest τ such that Hopf bifurcation occurs.

If (H_5) holds, Eq (2.20) has two positive roots

$$s_n^\pm = \frac{1}{2}\left(-P_n \pm \sqrt{R_n}\right)$$

and Eq (2.15) has two pairs of purely imaginary roots $\pm \mathrm{i}\omega_n^\pm = \pm \mathrm{i}\sqrt{s_n^\pm}$. We have

$$\tau_{n,j}^\pm = \begin{cases} \frac{1}{\omega_n^\pm} \arccos C_n(\omega_n^\pm) + \frac{2j\pi}{\omega_n^\pm}, & \mathcal{S}_n(\omega_n^\pm) > 0, \\ -\frac{1}{\omega_n^\pm} \arccos C_n(\omega_n^\pm) + \frac{2(j+1)\pi}{\omega_n^\pm}, & \mathcal{S}_n(\omega_n^\pm) < 0, \end{cases} \tag{2.22}$$

for $n \in \mathbb{N}_0$, $j \in \mathbb{N}_0$. Differentiating Eq (2.15) with respect to τ, we obtain

$$\operatorname{sign}\left\{\frac{\mathrm{d}(\mathrm{Re}\lambda)}{\mathrm{d}\tau}\right\}\Big|_{\lambda=\mathrm{i}\omega_n^\pm} = \operatorname{sign}\left\{\frac{2\omega_n^{\pm^2} + P_n}{m^2\omega_n^{\pm^2} + C_n^2}\right\} = \operatorname{sign}\left\{\frac{\pm\sqrt{R_n}}{m^2\omega_n^{\pm^2} + C_n^2}\right\},$$

then we have

$$\operatorname{sign}\left\{\frac{\mathrm{d}(\mathrm{Re}\lambda)}{\mathrm{d}\tau}\Big|_{\tau=\tau_{n,j}^{-}}\right\}<0,\quad \operatorname{sign}\left\{\frac{\mathrm{d}(\mathrm{Re}\lambda)}{\mathrm{d}\tau}\Big|_{\tau=\tau_{n,j}^{+}}\right\}>0.$$

Denote

$$\mathfrak{S}_2=\{n\in\mathbb{N}_0|\ (H_5)\text{ holds}\}.$$

For any $n\in\mathfrak{S}_2$, define $\tau_*=\min\limits_{n\in\mathfrak{S}_2}\left\{\tau_{n,0}^{+},\tau_{n,0}^{-}\right\}$.

Theorem 2.6. *Assume that (H_1) and (H_2) hold and $d_1<d_1^*$. Then, the following statements are true.*

(i) If (H_3) holds, $E_3(u_3,v_3)$ is locally asymptotically stable for all $\tau>0$.

(ii) If (H_4) holds, $E_3(u_3,v_3)$ is locally asymptotically stable when $\tau\in[0,\tau_*)$ and it is unstable when $\tau>\tau_*$. System (1.3) *undergoes Hopf bifurcation at $E_3(u_3,v_3)$ when $\tau=\tau_{n,j}$ $(n\in\mathfrak{S}_1)$.*

(iii) If (H_5) holds, $E_3(u_3,v_3)$ is locally asymptotically stable when

$$\tau\in[0,\tau_*)\bigcup(\tau_1,\tau_2)\bigcup\cdots\bigcup(\tau_{m-1},\tau_m)$$

and unstable when

$$\tau\in(\tau_*,\tau_1)\bigcup(\tau_2,\tau_3)\bigcup\cdots\bigcup(\tau_m,+\infty),$$

where $m\in\mathbb{N}$ and $\tau_*<\tau_1<\tau_2<\cdots<\tau_m\in\left\{\tau_{n,j}^{\pm}\Big|\,n\in\mathfrak{S}_2,j\in\mathbb{N}_0\right\}$. System (1.3) *undergoes Hopf bifurcation at $E_3(u_3,v_3)$ when $\tau=\tau_{n,j}^{\pm}$ $(n\in\mathfrak{S}_2)$.*

Combining Theorem 2.5 and Theorem 2.6, one can obtain the existence of Turing-Hopf bifurcation.

Theorem 2.7. *Assume that (H_1) and (H_2) hold. $E_3(u_3,v_3)$ is locally asymptotically stable when $\tau<\tau_*$ and $d_1<d_1^*$. System* (1.3) *undergoes a Turing-Hopf bifurcation at $E_3(u_3,v_3)$ when $(\tau,d_1)=(\tau_*,d_1^*)$.*

3. Normal form of Turing-Hopf bifurcation

In this section, we calculate the normal form of system (1.3) when a Turing-Hopf bifurcation occurs at $(\tau,d_1)=(\tau_*,d_1^*)$.

Let $\hat{u}(x,t)=u(x,\tau t)-u_3$, $\hat{v}(x,t)=v(x,\tau t)-v_3$ and drop the hats. System (1.3) can be written as

$$\frac{\partial}{\partial t}\begin{pmatrix}u(x,t)\\v(x,t)\end{pmatrix}=\tau\left[(D\Delta+L_1)\begin{pmatrix}u(x,t)\\v(x,t)\end{pmatrix}+L_2\begin{pmatrix}u(x,t-1)\\v(x,t-1)\end{pmatrix}+\begin{pmatrix}f_1\\g_1\end{pmatrix}\right],\tag{3.1}$$

where

$$\begin{aligned}f_1(\phi_1,\phi_2)=&\frac{1}{2}\left[a_1\phi_1^2(0)+2a_2\phi_1(0)\phi_2(0)\right]+\frac{1}{6}\left[a_3\phi_1^3(0)+3a_4\phi_1^2(0)\phi_2(0)\right]+O(4),\\ g_1(\phi_1,\phi_2)=&\frac{1}{2}\left[b_1\phi_1^2(-1)+2b_2\phi_1(-1)\phi_2(0)+2b_3\phi_1(-1)\phi_2(-1)+b_4\phi_2^2(0)+2b_5\phi_2(0)\phi_2(-1)\right]\\&+\frac{1}{6}\left[b_6\phi_1^3(-1)+3b_7\phi_1^2(-1)\phi_2(0)+3b_8\phi_1^2(-1)\phi_2(-1)+3b_9\phi_1(-1)\phi_2^2(0)\right.\\&\left.+6b_{10}\phi_1(-1)\phi_2(0)\phi_2(-1)+b_{11}\phi_2^3(0)+3b_{12}\phi_2^2(0)\phi_2(-1)\right]+O(4),\end{aligned}$$

with $\phi_1, \phi_2 \in C := C([-1, 0], X_{\mathbb{C}})$,

$$
\begin{aligned}
&a_1 = \frac{2\beta v_3}{(\beta+u_3)^3} - 2, \quad a_2 = -\frac{\beta}{(\beta+u_3)^2}, \quad a_3 = -\frac{6\beta v_3}{(\beta+u_3)^4}, \quad a_4 = \frac{2\beta}{(\beta+u_3)^3},\\
&b_1 = \frac{-2\alpha\beta v_3^2}{(\beta+u_3)^3(\delta+v_3)}, \quad b_2 = \frac{\alpha\beta\delta v_3}{(\beta+u_3)^2(\delta+v_3)^2}, \quad b_3 = \frac{\alpha\beta v_3}{(\beta+u_3)^2(\delta+v_3)}, \quad b_4 = \frac{-2\alpha\delta u_3 v_3}{(\beta+u_3)(\delta+v_3)^3},\\
&b_5 = \frac{\alpha\delta u_3}{(\beta+u_3)(\delta+v_3)^2}, \quad b_6 = \frac{6\alpha\beta v_3^2}{(\beta+u_3)^4(\delta+v_3)}, \quad b_7 = \frac{-2\alpha\beta\delta v_3}{(\beta+u_3)^3(\delta+v_3)^2}, \quad b_8 = \frac{-2\alpha\beta v_3}{(\beta+u_3)^3(\delta+v_3)},\\
&b_9 = \frac{-2\alpha\beta\delta v_3}{(\beta+u_3)^2(\delta+v_3)^3}, \quad b_{10} = \frac{\alpha\beta\delta}{(\beta+u_3)^2(\delta+v_3)^2}, \quad b_{11} = \frac{6\alpha\delta u_3 v_3}{(\beta+u_3)(\delta+v_3)^4}, \quad b_{12} = \frac{-2\alpha\delta u_3}{(\beta+u_3)(\delta+v_3)^3}.
\end{aligned} \tag{3.2}
$$

Setting $(\tau, d_1) = \left(\tau_* + \alpha_1, d_1^* + \alpha_2\right)$, system (3.1) undergoes a Turing-Hopf bifurcation when $(\alpha_1, \alpha_2) = (0, 0)$. System (3.1) can be rewritten as

$$
\frac{\mathrm{d}U(t)}{\mathrm{d}t} = D_0 \Delta U(t) + L_0 U^t + \widetilde{F}\left(\alpha, U^t\right), \tag{3.3}
$$

where

$$
\begin{aligned}
&D_0 = \tau_* \begin{pmatrix} d_1^* & \\ & d_2 \end{pmatrix}, \quad L_0 U^t = \tau_* \left[L_1 U^t(0) + L_2 U^t(-1)\right],\\
&\widetilde{F}\left(\alpha, U^t\right) = \left(\alpha_1 D_1^{(1,0)} + \alpha_2 D_1^{(0,1)}\right) \Delta U(t) + \left(\alpha_1 L_1^{(1,0)} + \alpha_2 L_1^{(0,1)}\right) U^t + F\left(\alpha, U^t\right).
\end{aligned}
$$

Here

$$
\begin{aligned}
&D_1^{(1,0)} = \begin{pmatrix} d_1^* & \\ & d_2 \end{pmatrix}, \quad D_1^{(0,1)} = \begin{pmatrix} \tau_* & \\ & 0 \end{pmatrix}, \quad L_1^{(1,0)} U^t = L_1 U^t(0) + L_2 U^t(-1),\\
&L_1^{(0,1)} U^t = 0, \quad F\left(\alpha, U^t\right) = (\tau_* + \alpha_1) \begin{pmatrix} f_1(\phi_1, \phi_2) \\ g_1(\phi_1, \phi_2) \end{pmatrix},
\end{aligned}
$$

with L_1, L_2 are defined in (2.14). Consider the linearized system of (3.3)

$$
\frac{\mathrm{d}U(t)}{\mathrm{d}t} = D_0 \Delta U(t) + L_0 U^t. \tag{3.4}
$$

Extend the phase space C to

$$
\mathcal{BC} := \left\{ \psi : [-1, 0] \to X_{\mathbb{C}} | \, \psi \text{ is continuous on } [-1, 0), \exists \lim_{\theta \to 0^-} \psi(\theta) \in X_{\mathbb{C}} \right\}.
$$

Equation (3.4) can be rewritten as an abstract ordinary differential equation on $\mathcal{BC}$

$$
\frac{\mathrm{d}U(t)}{\mathrm{d}t} = A U^t + X_0 \mathcal{F}\left(\alpha, U^t\right), \tag{3.5}
$$

where

$$
X_0 = \begin{cases} 0, & \theta \in [-1, 0), \\ I, & \theta = 0, \end{cases}
$$

and A is the infinitesimal generator of the semigroup of solution maps of the linear Eq (3.4), defined by $A : C_0^1 \bigcap \mathcal{BC} \to \mathcal{BC}$, $A\varphi = \dot{\varphi} + X_0[D_0 \Delta\varphi(0) + L_0(\varphi) - \dot{\varphi}(0)]$ with

$\mathrm{dom}(A) = \{\varphi \in C | \dot{\varphi} \in C, \varphi(0) \in \mathrm{dom}(\Delta)\}$. Denote $\eta_k \in BV([-1,0], \mathbb{C}^{2\times 2})$ to be the function of bounded variation defined on $[-1,0]$, such that

$$-\frac{n_k^2}{l^2} D_0\psi(0) + L_0\psi = \int_{-1}^{0} d\eta_k(\theta)\psi(\theta), \quad \psi \in C.$$

The adjoint bilinear form on $C^* \times \mathcal{B}C$ is defined by

$$(\psi, \varphi)_k = \psi(0)\varphi(0) - \int_{-1}^{0}\int_{0}^{\theta} \psi(\xi-\theta)\eta_k(\theta)\varphi(\xi)d\xi, \ \psi \in C^*, \ \varphi \in \mathcal{B}C,$$

where $k = 1, 2$, and $C^* \triangleq C([0,1]; \mathbb{C}^2)$.

From Theorem 2.7, system (3.4) has a pair of pure imaginary eigenvalues $\pm i\omega_0\tau_*$ and a zero eigenvalue at the Turing-Hopf bifurcation point, and all the other eigenvalues have negative real parts. Choose

$$\Phi_1(\theta) = \left(\phi_1(\theta), \overline{\phi}_1(\theta)\right), \quad \Phi_2(\theta) = \phi_2(\theta), \quad \Psi_1(s) = \left(\psi_1(s), \overline{\psi}_1(s)\right)^T, \quad \Psi_2(s) = \psi_2(s)$$

as the basis of the generalized eigenspace of A_i and A_i^* $(i = 1, 2)$, satisfying

$$A_i\Phi_i = \Phi_i B_i, \quad A_i^*\Psi_i = B_i\Psi_i, \quad (\Psi_i, \Phi_i)_i = I, \quad i = 1, 2,$$

where $B_1 = \mathrm{diag}\{i\omega_0\tau_*, -i\omega_0\tau_*\}$, $B_2 = 0$. Denote

$$\Phi(\theta) = (\Phi_1(\theta), \Phi_2(\theta)), \quad \Psi(s) = (\Psi_1(s), \Psi_2(s))^T.$$

By some calculations, we have

$$\begin{aligned} &\phi_1(\theta) = e^{i\omega_0\tau_*\theta}(1, k_1)^T, \qquad \phi_2(\theta) = (1, k_3)^T, \qquad \theta \in [-1, 0), \\ &\psi_1(s) = e^{-i\omega_0\tau_* s}M_1(1, k_2), \quad \psi_2(s) = M_3(1, k_4), \quad s \in [0, 1], \end{aligned}$$

where

$$\begin{aligned} &k_1 = \frac{i\omega_0\tau_* - a_{11}}{a_{12}}, \quad k_2 = \frac{i\omega_0\tau_* - a_{11}}{b_{21}e^{-i\omega_0\tau_*}}, \quad k_3 = \frac{d_1 n_2^2 - a_{11}l^2}{a_{12}l^2}, \quad k_4 = \frac{d_1 n_2^2 - a_{11}l^2}{b_{21}l^2}, \\ &M_1 = \frac{e^{i\omega_0\tau_*}}{e^{i\omega_0\tau_*}(k_1k_2 + 1) + \tau_* k_2\left[b_{21} + mk_1\right]}, \quad M_2 = \frac{1}{k_3k_4 + 1 + \tau_* k_4\left(mk_3 + b_{21}\right)}. \end{aligned}$$

Decomposing $\mathcal{B}C$ into a center subspace $\mathcal{P}$ and its orthocomplement space $\ker\pi$:

$$\mathcal{B}C = \mathcal{P} \oplus \ker\pi,$$

where

$$\mathcal{P} = \mathrm{span}\{\phi_1(\theta)\beta_{n_1}, \ \overline{\phi}_1(\theta)\beta_{n_1}, \ \phi_2(\theta)\beta_{n_2}\},$$

and $\pi : \mathcal{B}C \to \mathcal{P}$ is the projection operator defined by

$$\pi\varphi = \sum_{k=1}^{2} \Phi_k(\Psi_k, \langle\varphi(\cdot), \beta_{n_k}\rangle)_k\beta_{n_k},$$

where $\beta_{n_k}^1 = (\beta_{n_k}, 0)^T, \beta_{n_k}^2 = (0, \beta_{n_k})^T$ and $\langle \cdot, \beta_{n_k} \rangle = \left\langle \cdot, \beta_{n_k}^1 + \beta_{n_k}^2 \right\rangle$. Therefore, $U^t \in \mathcal{BC}$ can be composed as

$$U^t(\theta) = \phi_1(\theta) z_1(t) \beta_{n_1} + \overline{\phi}_1(\theta) \bar{z}_1(t) \beta_{n_1} + \phi_2(\theta) z_2(t) \beta_{n_2} + y_t(\theta) \triangleq \Phi(\theta) z_x(t) + y_t(\theta), \tag{3.6}$$

where

$$z_k(t) = (\Psi_k, \langle U^t(\cdot), \beta_{n_k} \rangle)_k, \quad y_t(\theta) \in C_0^1 \bigcap \ker\pi := Q^1.$$

System (3.4) on $\mathcal{BC}$ can be expressed as a system on $\mathbb{C}^3 \times \ker\pi$

$$\begin{cases} \dot{z}_1 = \mathrm{i}\omega_0 \tau_* z_1 + \psi_1(0) \left\langle \mathcal{F}\left(\alpha, \Phi(\theta) z_x(t) + y_t(\theta)\right), \beta_{n_1} \right\rangle, \\ \dot{\bar{z}}_1 = -\mathrm{i}\omega_0 \tau_* \bar{z}_1 + \bar{\psi}_1(0) \left\langle \mathcal{F}\left(\alpha, \Phi(\theta) z_x(t) + y_t(\theta)\right), \beta_{n_1} \right\rangle, \\ \dot{z}_2 = \psi_2(0) \left\langle \mathcal{F}\left(\alpha, \Phi(\theta) z_x(t) + y_t(\theta)\right), \beta_{n_2} \right\rangle, \\ \dot{y} = A_1 y + (I - \pi) X_0 \mathcal{F}\left(\alpha, \Phi(\theta) z_x(t) + y_t(\theta)\right), \end{cases}$$

where A_1 is the restriction of A on $Q^1 \subset \ker\pi \to \ker\pi$, $A_1\varphi = A\varphi$ for $\varphi \in Q^1$.

In the following, we apply the algorithm given by An and Jiang [19] and obtain normal form truncated to the third order for the Turing-Hopf bifurcation

$$\begin{cases} \dot{z}_1 = \mathrm{i}\omega_0 \tau_* z_1 + \frac{1}{2} f_{\alpha_1 z_1}^{11} \alpha_1 z_1 + \frac{1}{2} f_{\alpha_2 z_1}^{11} \alpha_2 z_1 + \frac{1}{6} g_{210}^{11} z_1^2 \bar{z}_1 + \frac{1}{6} g_{102}^{11} z_1 z_2^2, \\ \dot{\bar{z}}_1 = -\mathrm{i}\omega_0 \tau_* \bar{z}_1 + \frac{1}{2} \overline{f_{\alpha_1 z_1}^{11}} \alpha_1 \bar{z}_1 + \frac{1}{2} \overline{f_{\alpha_2 z_1}^{11}} \alpha_2 \bar{z}_1 + \frac{1}{6} \overline{g_{210}^{11}} z_1 \bar{z}_1^2 + \frac{1}{6} \overline{g_{102}^{11}} \bar{z}_1 z_2^2, \\ \dot{z}_2 = \frac{1}{2} f_{\alpha_1 z_2}^{13} \alpha_1 z_2 + \frac{1}{2} f_{\alpha_2 z_2}^{13} \alpha_2 z_2 + \frac{1}{6} g_{111}^{13} z_1 \bar{z}_1 z_2 + \frac{1}{6} g_{003}^{13} z_2^3. \end{cases} \tag{3.7}$$

The coefficients of quadratic and cubic terms in (3.7) are in Appendix.

Making the cylindrical coordinate transformation by

$$z_1 = \mathcal{R}\cos\theta + \mathrm{i}\mathcal{R}\sin\theta_1, \ \bar{z}_1 = \mathcal{R}\cos\theta - \mathrm{i}\mathcal{R}\sin\theta_1, \ z_2 = \mathcal{V},$$

where $\mathcal{R} > 0$ and $\mathcal{V} > 0$. Re-scaling the variables with

$$\rho = \sqrt{\frac{|\mathrm{Re}(g_{210}^{11})|}{6}}\mathcal{R}, \quad \eta = \sqrt{\frac{|g_{003}^{13}|}{6}}\mathcal{V}, \quad \widehat{t} = \frac{t}{\varepsilon}, \quad \varepsilon = \mathrm{sign}\left(\mathrm{Re}\left(g_{210}^{11}\right)\right)$$

and dropping the hats, system (3.7) is transformed into

$$\begin{cases} \dot{\rho} = \rho[\epsilon_1(\alpha_1, \alpha_2) + \rho^2 + b_0\eta^2], \\ \dot{\eta} = \eta[\epsilon_2(\alpha_1, \alpha_2) + c_0\rho^2 + d_0\eta^2], \end{cases} \tag{3.8}$$

where

$$\begin{aligned} \epsilon_1(\alpha_1, \alpha_2) &= \frac{\varepsilon}{2}\left[\mathrm{Re}(f_{\alpha_1 z_1}^{11})\alpha_1 + \mathrm{Re}(f_{\alpha_2 z_1}^{11})\alpha_2\right], \\ \epsilon_2(\alpha_1, \alpha_2) &= \frac{\varepsilon}{2}\left[f_{\alpha_1 z_2}^{13}\alpha_1 + f_{\alpha_2 z_2}^{13}\alpha_2\right], \\ b_0 &= \frac{\varepsilon \mathrm{Re}(g_{102}^{11})}{|g_{003}^{13}|}, \quad c_0 = \frac{\varepsilon g_{111}^{13}}{|\mathrm{Re}(g_{210}^{11})|}, \quad d_0 = \frac{\varepsilon g_{003}^{13}}{|g_{003}^{13}|} = \pm 1. \end{aligned}$$

According to Guckenheimer and Holmes [28], there are twelve distinct types of unfoldings for system (3.8) according to the signs of b_0, c_0, d_0 and $d_0 - b_0c_0$ (see Table 1).

Table 1. The twelve unfoldings of system (3.7).

Case	Ia	Ib	II	III	IVa	IVb	V	VIa	VIb	VIIa	VIIb	VIII
d_0	+1	+1	+1	+1	+1	+1	+1	−1	−1	−1	−1	−1
c_0	+	+	+	−	−	−	+	+	+	−	−	−
d_0	+	+	−	+	−	−	+	−	−	+	+	−
$d_0 - b_0c_0$	+	−	+	+	+	−	−	+	−	+	−	−

4. Numerical simulations

In the following, we carry out numerical simulations to support our theoretical results obtained in the previous sections and symbolic mathematical software Matlab is used to plot numerical graphs. The delayed reaction-diffusion system (1.3) is numerically solved by transforming the continuous system to discrete system using discretization of time and space. In the discrete system, the Laplacian describing diffusion is calculated by using finite differences scheme with central differences, and the time evolution is solved by using the forward (explicit) Euler method (with the Courant-Friedrichs-Lewy (CFL) condition satisfied) [29].

For the numerical simulations, we choose hypothetical parameter data to verify the theoretical results and demonstrate possible dynamical behaviours. Thus, we vary the parameters to verify the conditions for the occurrence of bifurcations, such as Turing bifurcation, Hopf bifurcation and Turing-Hopf bifurcation. Meanwhile, we observe the effect of varying diffusive coefficient, delay and Allee effect constant on the dynamics of system. Therefore, similar to Sen et al. [10] and Ghosh et al. [30], we choose the parameters in some range (see Table 2).

Table 2. Value of the parameters for numerical simulations.

Parameter	Turing bifurcation	Hopf bifurcation	Turing-Hopf bifurcation
α	1.2	1.2	1.2
β	0.3	0.3	0.3
d_1	[18.7, 19.2]	10	[15, 18.4]
d_2	0.5	0.5	0.5
δ	0.1	[0.1, 0.11]	0.1
l	6	6	6
m	0.58	0.58	0.58
τ	/	[0, 30]	[0.15, 0.75]

4.1. Turing instability

In this subsection, we choose $\delta = 0.1$ such that (H_1) and (H_2) hold. Taking d_1 as the bifurcation parameter, we carry out numerical simulations for non delayed system (2.5) and illustrate the pattern formulations induced by Turing bifurcation.

By direct calculation, we have $a_{22}l^2/d_2 = 8.1517$. Thus, $d_1(n^2) > 0$ if $n^2 < 8.1517$. Figure 2 shows the relationship between d_1 and n according to (2.10). It indicates that $q^* \approx 1.9898$, $N^* = 2$. Thus, from (2.11), we have $d_1^* = d_1\left(N^{*^2}\right) = d_1(2^2) = 18.7569$. Therefore, from Theorem 2.5, we conclude

that $E_3(0.4511, 0.4123)$ of non delayed system (2.5) is stable when $d_1 < d_1^*$ and unstable when $d_1 > d_1^*$. Figure 3 demonstrates that E_3 is stable for $d_1 = 18.7 < d_1^*$. For $d_1 = 19.2 > d_1^*$, $E_3(0.4511, 0.4123)$ is unstable, which is shown in Figure 4.

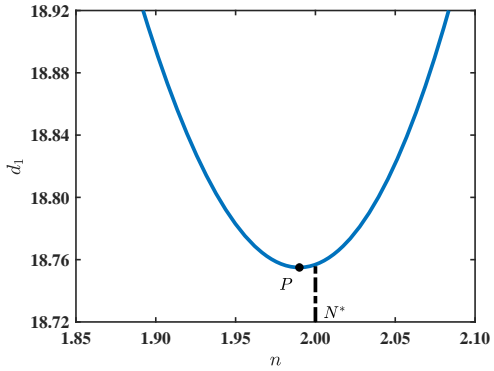

Figure 2. The diagram of $d_1(n^2)$ on the (n, d_1) plane.

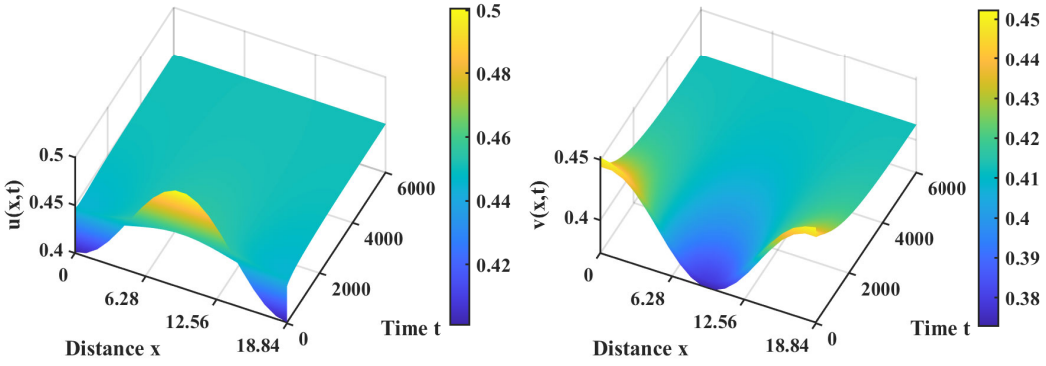

(a) **(b)**

Figure 3. The positive equilibrium $E_3(u_3, v_3)$ is stable when $d_1 = 18.5 < d_1^*$.

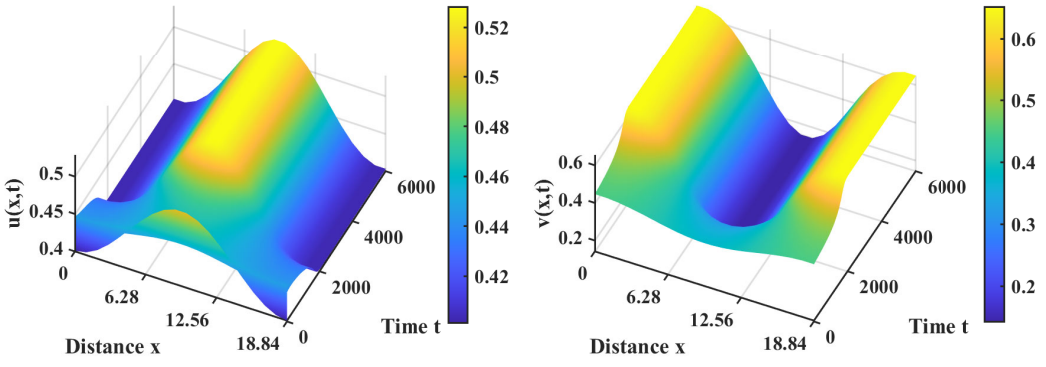

(a) **(b)**

Figure 4. The positive equilibrium $E_3(u_3, v_3)$ is unstable induced by Turing bifurcation when $d_1 = 19.2 > d_1^*$.

For the numerical simulations in Figures 3 and 4, the initial value functions are both $u(x,0) = 0.45 - 0.05\cos\left(\frac{1}{3}x\right)$, $v(x,0) = 0.41 + 0.04\cos\left(\frac{1}{3}x\right)$.

4.2. Hopf bifurcation

In this section, we reveal the effect of τ on the dynamics of system (1.3). Thus, we fix $d_1 = 10 < d_1^*$ such that $E_3(u_3, v_3)$ is stable for $\tau = 0$. We find that the strength of Allee effect has an important role in the occurrence of Hopf bifurcation.

Choose $\delta = 0.1$ such that the strength of Allee effect is low. We can verify that (H_1) and (H_2) hold. Moreover, (H_4) holds only for $n = 0$. Then, Eq (2.20) has a unique positive root s_0^+. From (2.21), the critical value of Hopf bifurcation is $\tau_* = 0.1571 = \tau_{0,0}$. From Theorem 2.6 (ii), the positive equilibrium $E_3(0.4511, 0.4123)$ is locally asymptotically stable when $\tau = 0.15 < \tau_*$ and unstable when $\tau = 1.5 > \tau_*$.

Table 3. Critical values of Hopf bifurcation $\tau_{n,j}^{\pm}$.

	$j = 0$	$j = 1$	$j = 2$	$j = 3$
$n = 0$	$\tau_{0,0}^+ = 0.7921$	$\tau_{0,1}^+ = 24.2091$	$\tau_{0,2}^+ = 47.6261$	$\tau_{0,3}^+ = 71.0431$
$n = 0$	$\tau_{0,0}^- = 3.7313$	$\tau_{0,1}^- = 38.7605$	$\tau_{0,2}^- = 73.7898$	$\tau_{0,3}^- = 108.8190$

When δ increases to $\delta = 0.105$, (H_1) and (H_2) hold. (H_5) holds only for $n = 0$, Eq (2.20) has two positive roots $s_0^{\pm}$. The critical value of Hopf bifurcation can be obtained (see Table 3), and we can get from (2.22) that

$$\tau_{0,0}^+ < \tau_{0,0}^- < \tau_{0,1}^+ < \tau_{0,1}^- < \tau_{0,2}^+ < \tau_{0,3}^+ < \tau_{0,2}^- < \tau_{0,3}^-.$$

From Theorem 2.6 (iii), the positive equilibrium $E_3(0.4639, 0.4095)$ is locally asymptotically stable when $\tau \in \left[0, \tau_{0,0}^+\right) \bigcup \left(\tau_{0,0}^-, \tau_{0,1}^+\right)$ and unstable when $\tau \in \left(\tau_{0,0}^+, \tau_{0,0}^-\right) \bigcup \left(\tau_{0,1}^+, +\infty\right)$. The delay τ may lead to stability switches with an intermediate strength of Allee effect, and there are two stability switches for system (1.3). Figures 5 and 7 show that $E_3(0.4639, 0.4095)$ is stable for $\tau = 0.5 \in \left[0, \tau_{0,0}^+\right)$ and $\tau = 10 \in \left(\tau_{0,0}^-, \tau_{0,1}^+\right)$, respectively. For $\tau = 3 \in \left(\tau_{0,0}^+, \tau_{0,0}^-\right)$ and $\tau = 30 \in \left(\tau_{0,1}^+, +\infty\right)$, $E_3(0.4639, 0.4095)$ is unstable (see Figures 6 and 8).

When δ is further increased to $\delta = 0.11$, we can verify (H_1), (H_2) and (H_3) hold. From Theorem 2.6 (i), $E_3(0.4776, 0.4062)$ is locally asymptotically stable for all $\tau > 0$.

4.3. Spatiotemporal patterns near the Turing-Hopf bifurcation point

In this section, we reveal the complex spatiotemporal dynamics near the Turing-Hopf bifurcation point (τ_*, d_1^*). Fix $\delta = 0.1$, and choose d_1 and τ as bifurcation parameters.

From (2.11) and (2.21), we have $\tau_* = 0.1571$, $d_1^* = 18.7569$. System (1.3) undergoes a Turing-Hopf bifurcation at $E_3(u_3, v_3)$ when $(\tau, d_1) = (\tau_*, d_1^*)$.

After calculation, we can obtain the coefficients in (3.8), where

$$\begin{aligned} &\epsilon_1 = -3.4272 \times 10^{-3}\alpha_1, \quad \epsilon_2 = -4.3221 \times 10^{-4}\alpha_2, \\ &b_0 = 4.576563, \quad c_0 = -0.714188, \quad d_0 = -1, \quad d_0 - b_0c_0 = 2.268527. \end{aligned}$$

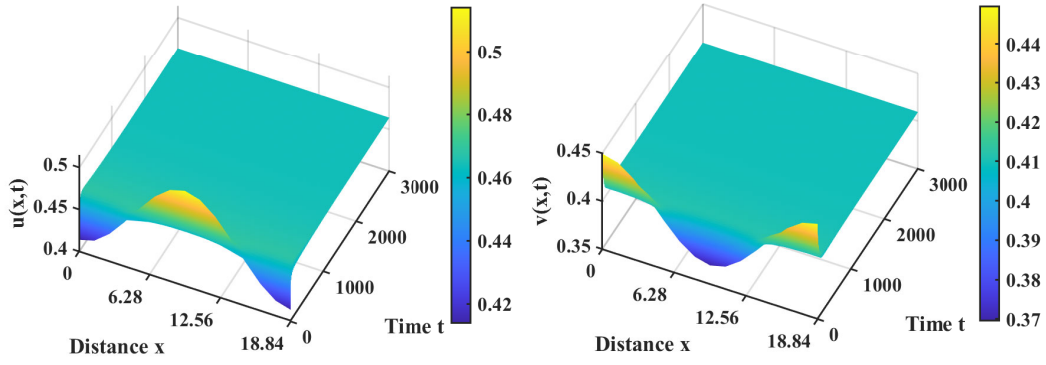

(a) **(b)**

Figure 5. The positive equilibrium $E_3(u_3, v_3)$ is locally asymptotically stable when $\tau = 0.5 \in \left[0, \tau^+_{0,0}\right)$.

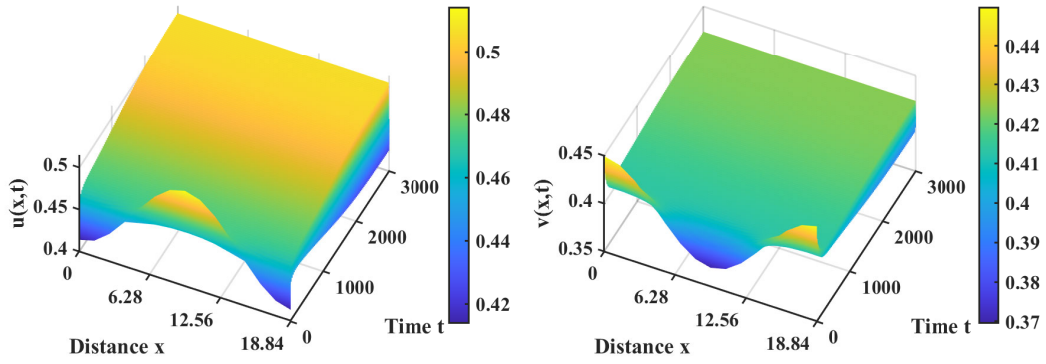

(a) **(b)**

Figure 6. There is a bifurcating periodic solution when $\tau = 3 \in \left(\tau^+_{0,0}, \tau^-_{0,0}\right)$.

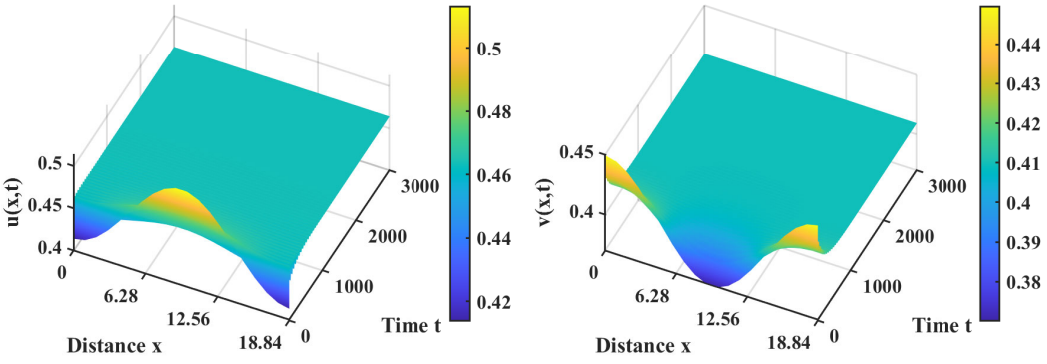

(a) **(b)**

Figure 7. The positive equilibrium $E_3(u_3, v_3)$ is locally asymptotically stable when $\tau = 10 \in \left(\tau^-_{0,0}, \tau^+_{0,1}\right)$.

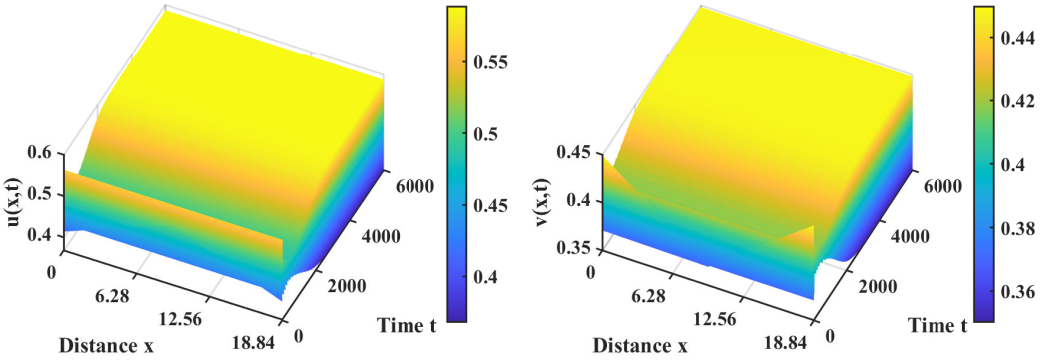

(a) **(b)**

Figure 8. There is a bifurcating periodic solution when $\tau = 30 \in \left(\tau_{0,1}^{+}, +\infty\right)$.

From Table 1, the unfolding system is of type VIa. System (3.8) can be written as

$$\begin{cases} \dot{\rho} = \rho\left(-3.4272 \times 10^{-3}\alpha_1 + \rho^2 + 4.576563\eta^2\right), \\ \dot{\eta} = \eta\left(-4.3221 \times 10^{-4}\alpha_2 - 0.714188\rho^2 - \eta^2\right). \end{cases} \tag{4.1}$$

By some simple calculations, we find that the system admits the following equilibria

$$\begin{aligned} A_0 =& (0,0), \\ A_1 =& \left(\sqrt{3.4272 \times 10^{-3}\alpha_1}, 0\right), \text{ for } \alpha_1 > 0, \\ A_2^{\pm} =& \left(0, \pm\sqrt{-4.3221 \times 10^{-4}\alpha_2}\right), \text{ for } \alpha_2 < 0, \\ A_3^{\pm} =& \left(\sqrt{-1.5110 \times 10^{-3}\alpha_1 - 8.7194 \times 10^{-4}\alpha_2}, \pm\sqrt{1.0790 \times 10^{-3}\alpha_1 + 1.9052 \times 10^{-4}\alpha_2}\right), \\ & \text{for } -1.5110 \times 10^{-3}\alpha_1 - 8.7194 \times 10^{-4}\alpha_2 > 0 \text{ and } 1.0790 \times 10^{-3}\alpha_1 + 1.9052 \times 10^{-4}\alpha_2 > 0. \end{aligned}$$

Since $\alpha_1 = \tau - \tau_*$, $\alpha_2 = d_1 - d_1^*$, the detailed bifurcation diagram in (τ, d_1) plane can be drawn (see Figure 9). There are six partial bifurcation curves:

$$\begin{aligned} &L_1 : \tau = 0.1571, \qquad L_2 : d_1 = 18.7569, \\ &T_1 : d_1 = -5.6634(\tau - 0.1571) + 18.7569, && (\tau > 0.1571), \\ &T_2 : d_1 = -5.6634(\tau - 0.1571) + 18.7569 + o(\tau - 0.1571), && (\tau > 0.1571), \\ &T_3 : d_1 = -2.4377(\tau - 0.1571) + 18.7569, && (\tau > 0.1571), \\ &T_4 : d_1 = -1.7329(\tau - 0.1571) + 18.7569, && (\tau > 0.1571), \end{aligned}$$

which divide (τ, d_1) plane into eight regions D_1-D_8. Furthermore, the spatiotemporal dynamics near the Turing-Hopf bifurcation point in D_1-D_8 can be described by Figure 10.

Notice that the zero equilibrium A_0 of (4.1) corresponds to the positive equilibrium $E_3(u_3, v_3)$ of the original system (1.3). A_1 in (4.1) corresponds to the spatially homogeneous periodic solution of the original system (1.3). The equilibria $A_2^{\pm}$ in (4.1) correspond to the steady state solutions of the original system (1.3). $A_3^{\pm}$ corresponds to spatially inhomogeneous periodic solutions. Periodic orbit of (4.1) corresponds to spatially inhomogeneous quasi-periodic solutions.

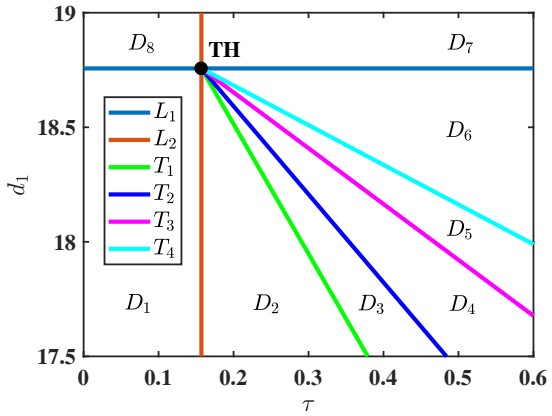

Figure 9. The bifurcation curves and partial bifurcation set near Turing-Hopf bifurcation point "TH" on the (τ, d_1) plane.

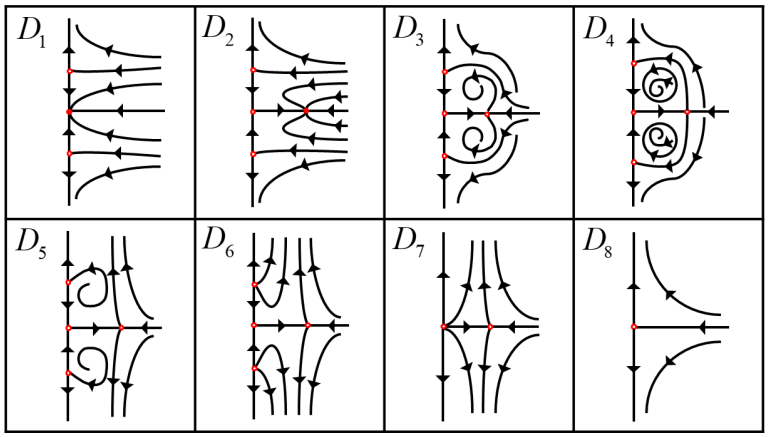

Figure 10. Distinct phase portrait near TH in D_1-D_8 corresponding to Figure 9.

In region D_1, system (4.1) has three equilibria: A_0 and $A_2^{\pm}$. A_0 is stable while other equilibria are unstable. This means that the positive equilibrium $E_3(u_3, v_3)$ is locally asymptotically stable as shown in Figure 11, when $\tau = 0.15$ and $d_1 = 15$ are chosen in D_1. The steady state solutions of (1.3) are unstable.

In region D_2, there are four equilibria of (4.1): A_0, A_1 and $A_2^{\pm}$. A_1 is stable while other equilibria are unstable. This means that system (1.3) has a stable spatially homogeneous periodic solution. Figure 12 illustrates the existence of a stable spatially homogeneous periodic solution when (τ, d_1) passes through Hopf bifurcation curve L_2 into D_2.

In region D_3, system (4.1) has six equilibria: A_0, A_1, $A_2^{\pm}$ and $A_3^{\pm}$. $A_3^{\pm}$ are stable while other equilibria are unstable. This means that there are two stable spatially inhomogeneous periodic solutions. Figure 13 illustrates the coexistence of two stable spatially inhomogeneous periodic solutions when (τ, d_1) enters D_3 from D_2.

In region D_4, there are six equilibria and two periodic orbit of system (4.1). This means that system (1.3) has two stable spatially inhomogeneous quasi-periodic solutions (see Figure 14).

In region D_5, system (4.1) has six equilibria: A_0, A_1, $A_2^{\pm}$ and $A_3^{\pm}$, which are all unstable. When the

parameter enters region D_5, two stable spatially inhomogeneous quasi-periodic solutions disappears. This means that the positive equilibrium $E_3(u_3, v_3)$, the spatially homogeneous periodic solution, two steady state solutions and two stable spatially inhomogeneous periodic solutions of system (1.3) are all unstable.

In region D_6, system (4.1) has four equilibria: A_0, A_1 and $A_2^{\pm}$, which are all unstable. This means that the positive equilibrium $E_3(u_3, v_3)$, the spatially homogeneous periodic solution and two steady state solutions of system (1.3) are all unstable.

In region D_7, there are two unstable equilibria A_0 and A_1 of system (1.3). This means that the positive equilibrium $E_3(u_3, v_3)$ and the spatially homogeneous periodic solution are all unstable.

In region D_8, system (4.1) has only one equilibrium A_0, which is a saddle. This means that the positive equilibrium $E_3(u_3, v_3)$ of system (1.3) is unstable.

For the numerical simulations, in Figures 11 and 12, the initial conditions are all $u(x, 0) = u_3 - 0.05\cos\left(\frac{1}{3}x\right)$, $v(x, 0) = v_3 + 0.04\cos\left(\frac{1}{3}x\right)$; the initial conditions are all $u(x, 0) = u_3 - 0.05\cos\left(\frac{1}{3}x\right)$, $v(x, 0) = v_3 + 0.04\cos\left(\frac{1}{3}x\right)$ in Figures 13(a)–(c) and 14(a)–(c) and the initial conditions are all $u(x, 0) = u_3 + 0.05\cos\left(\frac{1}{3}x\right)$, $v(x, 0) = v_3 - 0.04\cos\left(\frac{1}{3}x\right)$ in Figures 13(d)–(f) and 14(d)– (f).

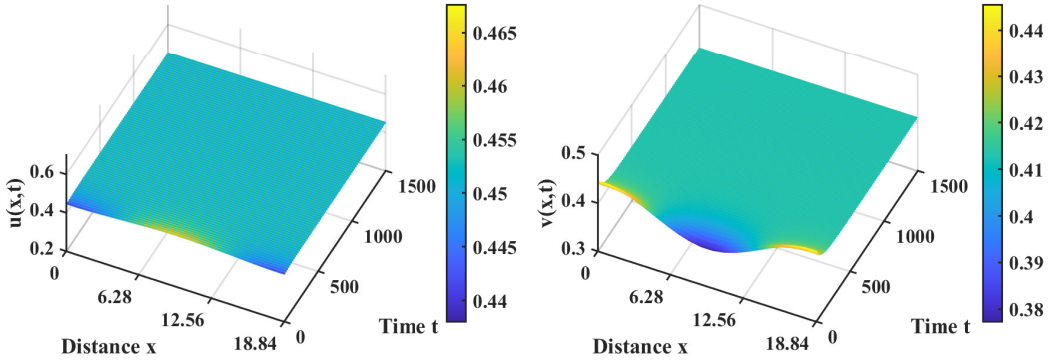

(a) **(b)**

Figure 11. The constant steady state for $(\tau, d_1) = (0.15, 15) \in D_1$.

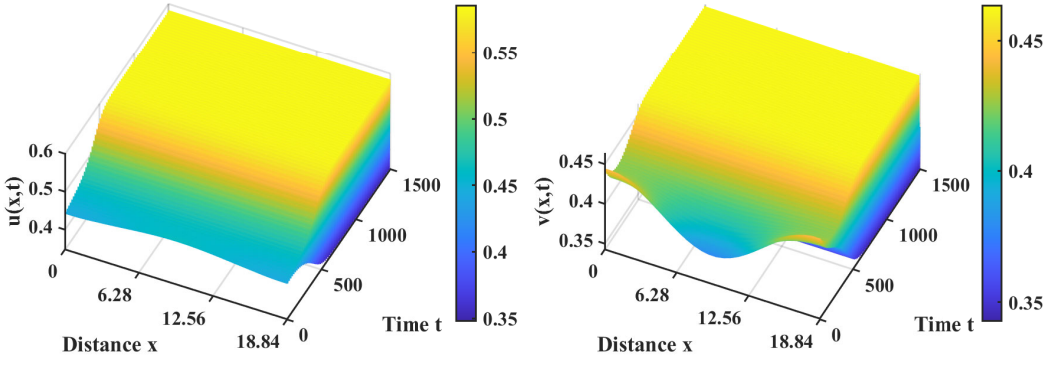

(a) **(b)**

Figure 12. The spatially homogeneous periodic solution for $(\tau, d_1) = (0.75, 15) \in D_2$.

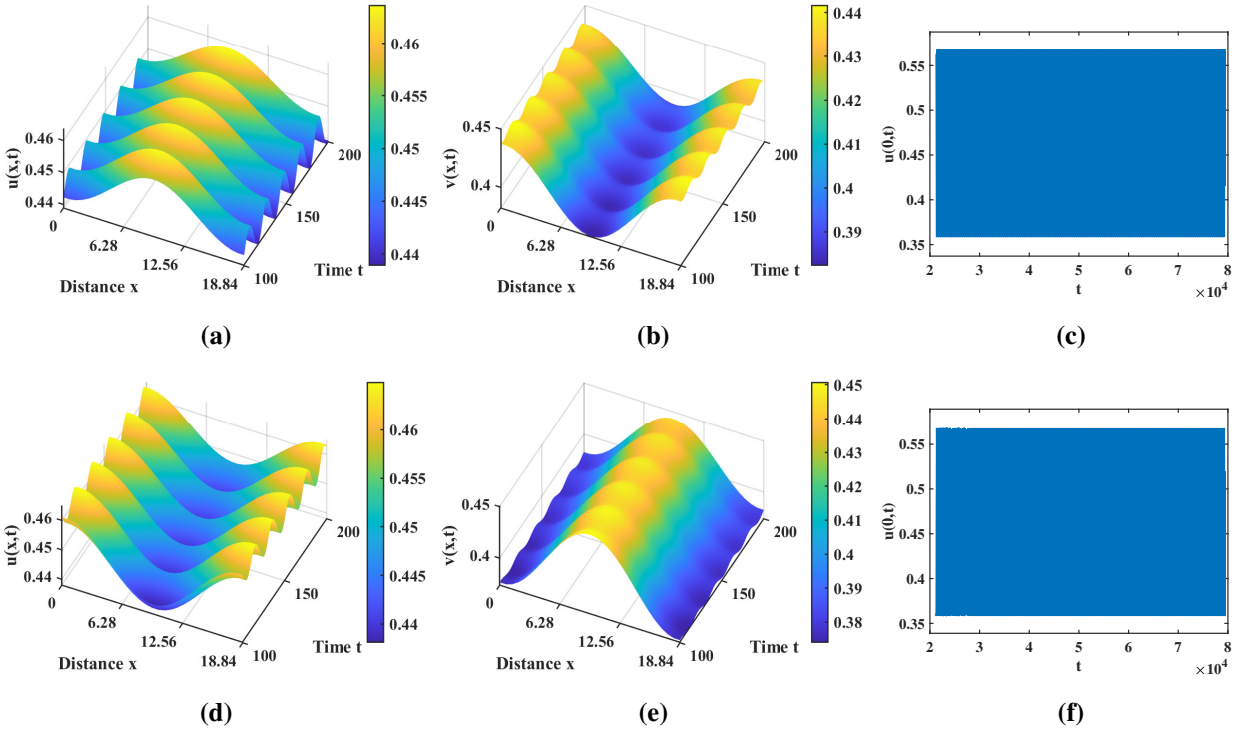

Figure 13. The spatially inhomogeneous periodic solutions coexist for $(\tau, d_1) = (0.35, 18) \in D_3$.

5. Conclusions and discussion

In this paper, we have considered a diffusive predator-prey model with digestion delay and Allee effect in predators.

First, we investigate the existence of equilibria. We find that the strength of Allee effect will affect the number of positive equilibria. When the strength of Allee effect $0 < \delta < \frac{[\alpha-(1-\beta)m]^2}{4m(\alpha-m)}$, system (1.3) has two positive equilibria $E_3(u_3, v_3)$ and $E_4(u_4, v_4)$. When the strength of Allee effect increases to a certain critical level $\delta = \frac{[\alpha-(1-\beta)m]^2}{4m(\alpha-m)}$, system (1.3) has a unique positive equilibrium $E_5(u_5, v_5)$ and undergoes saddle-node bifurcation. If the strength of Allee effect exceeds the critical value, system (1.3) has no positive equilibria. It is found that Allee effect in predators has a crucial role on the dynamical behavior of our system. From Theorem 2.1, we find that the Allee effect may impact the coexistence of predators and the prey. When the strength of Allee effect is high, the predators and the prey can not coexist, resulting in the extinction of the predator populations at low population densities, which is consistent with the findings of Li et al. [11]. Remark 2.2 tells us that the strength of Allee effect also influences the densities of the species. From the analysis of the stable equilibrium $E_3(u_3, v_3)$, the densities of predators and prey increases and decreases with the increasing strength of Allee effect.

For the non delayed system, we obtain the conditions for the stability and instability induced by diffusion of the positive equilibrium $E_3(u_3, v_3)$. For the delayed system, there are three distinct cases for the occurrence of Hopf bifurcation with different levels of Allee effect strength. If the strength of the Allee effect δ is low, digestion delay τ will alter the stability of the positive equilibrium $E_3(u_3, v_3)$

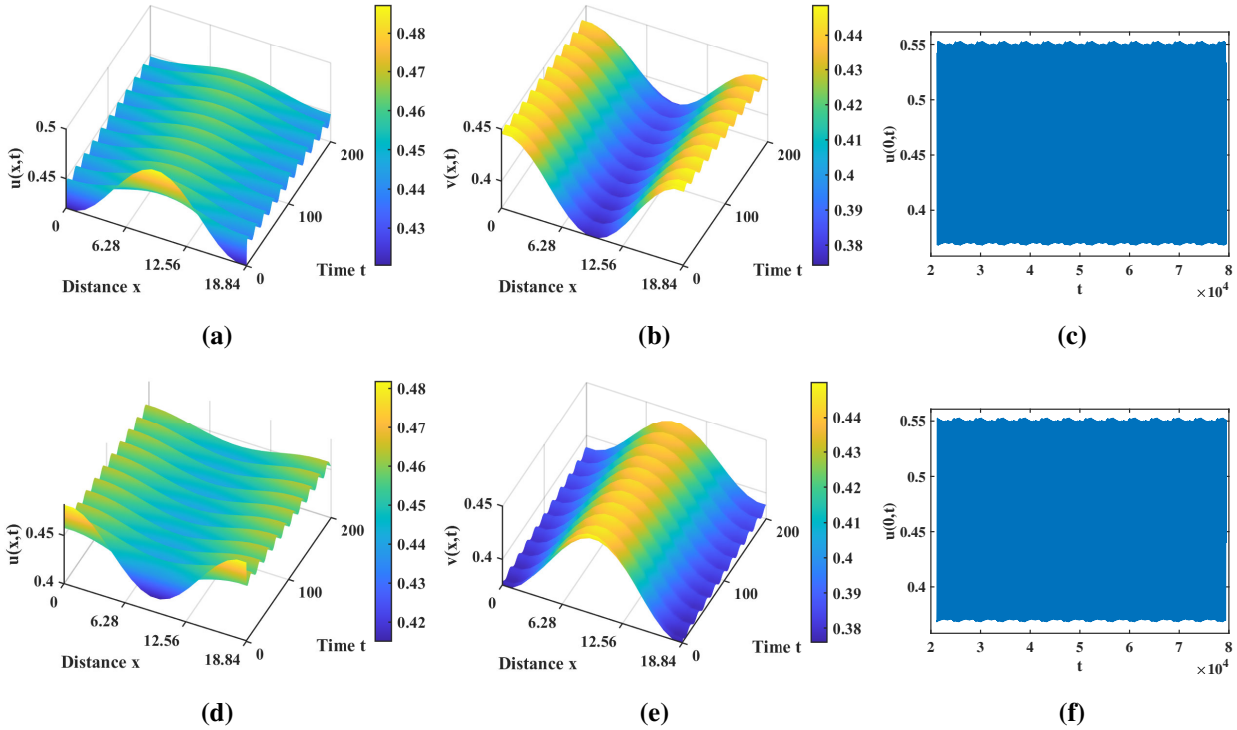

Figure 14. The spatially inhomogeneous quasi-periodic solutions coexist for $(\tau, d_1) = (0.25, 18.4) \in D_4$.

and induce Hopf bifurcation. When the strength of Allee effect δ increases to an intermediate value, digestion delay τ will induce Hopf bifurcation and stability switches. Finally, when the strength of Allee effect δ is high, Hopf bifurcation will not occur and the stability of the positive equilibrium $E_3(u_3, v_3)$ will not be changed.

Furthermore, we determine the conditions of Turing-Hopf bifurcation and calculate its normal form. Taking d_1 and τ as bifurcation parameters, the effects of diffusion and digestion delay are investigated. We derive normal forms truncated to the third order near Turing-Hopf bifurcation point (τ_*, d_1^*) and obtain the classification of dynamics. The parameter plane near the Turing-Hopf bifurcation can be divided into eight regions, each with clear dynamics. When the parameter (τ, d_1) is in region D_1, the positive equilibrium $E_3(u_3, v_3)$ is locally asymptotically stable. If $(\tau, d_1) \in D_2$, there is a stable spatially homogeneous periodic solution. When (τ, d_1) enters D_3 from D_2, there exist two stable spatially inhomogeneous periodic solutions. Two stable spatially inhomogeneous quasi-periodic solutions appear in D_4 and disappear in D_5. Using Turing-Hopf bifurcation, we can easily qualitatively classify dynamics on a two-parameter plane and understand the combined effects of diffusion and digestion delay on predator-prey interactions, which has important theoretical significance for environmental protection, endangered species protection and biodiversity protection.

In this paper, we explore the spatiotemporal dynamics of a predator-prey model with Allee effect in predators, applying the normal form theory of Turing-Hopf bifurcation extended by An et al. [19] and Jiang et al. [23]. Li et al. [11] mainly discussed the effect of delay on the dynamics, and it is shown that the model can possess multiple stability switches and a stable spatially heterogeneous periodic solution with mode-4 as delays vary. Wang et al. [25] studied local and global stability of the positive

equilibrium as well as Turing instability, and the rich Turing patterns are demonstrated by numerical simulations, including holes, stripes and spots patterns. In our paper, we focus on the joint effect of diffusion, delay and Allee effect on the dynamics through Turing bifurcation, Hopf bifurcation and Turing-Hopf bifurcation analysis. The findings of this study reveal the possibility of two stable spatially inhomogeneous periodic solutions and a spatially quasi-periodic solution, with different dynamics from those observed when both predator and prey populations exhibit Allee effect [27].

Most present research on prey-predator models has assumed that the biological parameters are exact. However, in reality, biological parameters can vary due to various reasons, which make the exact estimation of these parameters difficult. Ghosh et al. [30] considered interval number biological parameters in their study, which can capture the complex dynamics of predator-prey systems and enable simulation of the effect of different environmental factors. In this article, we carry out detailed bifurcation analysis on continuous-time model, such as Turing bifurcation, Hopf bifurcation and Turing-Hopf bifurcation. For discrete-time model, Naik et al. [31, 32] investigate the one-parameter and two-parameter bifurcations of a discrete-time prey-predator model, including the flip (period-doubling), generalized flip, Neimark-Sacker and strong resonance bifurcations.

We consider two species in the model and only consider interspecific competition for resources. When we consider a system with more species, prey species can sometimes indirectly depress each other by increasing the abundance of a shared natural enemy, which is called apparent competition [33, 34]. Taking these into account, the influence of the apparent competition on the spatiotemporal dynamics of the predator-prey model with Allee effect would be worth for further study. In addition, other ecological phenomena, such as hydra effects [35] and harvesting [36, 37], could offer intriguing possibilities for future research.

Use of AI tools declaration

The authors declare they have not used Artificial Intelligence (AI) tools in the creation of this article.

Acknowledgments

The work is supported by National Natural Science Foundation of China (grant no. 11901369, 12071268 and 11971281).

Conflict of interest

The authors declare there is no conflicts of interest.

References

1. A. J. Lotka, Elements of physical biology, *Nature*, **116** (1925), 461. https://doi.org/10.1038/116461b0
2. V. Volterra, Variations and fluctuations of the number of individuals in animal species living together, *ICES J. Mar. Sci.*, **3** (1928), 3–51. https://doi.org/10.1093/icesjms/3.1.3

3. S. Zhou, Y. Liu, G. Wang, The stability of predator-prey systems subject to the Allee effects, *Theor. Popul. Biol.*, **67** (2005), 23–31. https://doi.org/ 10.1016/j.tpb.2004.06.007
4. P. Aguirre, E. Gonzalez-Olivares, E. Saez, Three limit cycles in a Leslie-Gower predator-prey model with additive Allee effect, *SIAM J. Appl. Math.*, **69** (2009), 1244–1262. https://doi.org/10.1137/070705210
5. J. Wang, J. Shi, J. Wei, Predator-prey system with strong Allee effect in prey, *J. Math. Biol.*, **62** (2011), 291–331. https://doi.org/10.1007/s00285-010-0332-1
6. F. Courchamp, L. Berec, J. Gascoigne, *Allee Effects in Ecology and Conservation*, 1^{st} edition, Oxford University Press, New York, 2008. https://doi.org/10.1093/acprof:oso/9780198570301.001.0001
7. D. Thompson, I. Strange, M. Riddy, C. D. Duck, The size and status of the population of southern sea lions Otaria flavescens in the Falkland Islands, *Biol. Conserv.*, **121** (2005), 357–367. https://doi.org/10.1016/j.biocon.2004.05.008
8. A. Hurford, M. Hebblewhite, M. A. Lewis, A spatially explicit model for an Allee effect: Why wolves recolonize so slowly in Greater Yellowstone, *Theor. Popul. Biol.*, **70** (2006), 244–254. https://doi.org/10.1016/j.tpb.2006.06.009
9. J. L. Stenglein, T. L. Deelen, Demographic and component Allee effects in southern lake superior gray wolves, *PLoS One*, **11** (2016), e0150535. https://doi.org/10.1371/journal.pone.0150535
10. D. Sen, S. Ghorai, M. Banerjee, A. Morozov, Bifurcation analysis of the predator-prey model with the Allee effect in the predator, *J. Math. Biol.*, **84** (2022), 1–27. https://doi.org/10.1007/s00285-021-01707-x
11. S. Li, S. Yuan, Z. Jin, H. Wang, Bifurcation analysis in a diffusive predator-prey model with spatial memory of prey, Allee effect and maturation delay of predator, *J. Differ. Equation*, **357** (2023), 32–63. https://doi.org/10.1016/j.jde.2023.02.009
12. L. Anjos, M. I. Costa, R. C. Almeida, Rapid spread agents may impair biological control in a tritrophic food web with intraguild predation, *Ecol. Complex.*, **46** (2021), 100926. https://doi.org/10.1016/j.ecocom.2021.100926
13. D. Sen, S. Petrovskii, S. Ghorai, M. Banerjee, Rich bifurcation structure of prey-predator model induced by the Allee effect in the growth of generalist predator, *Int. J. Bifurcat. Chaos*, **30** (2020), 1–22. https://doi.org/10.1142/S0218127420500844
14. S. Rana, A. R. Bhowmick, S. Bhattacharya, Impact of prey refuge on a discrete time predator-prey system with Allee effect, *Int. J. Bifurcat. Chaos*, **24** (2014), 1450106. https://doi.org/10.1142/S0218127414501065
15. A. Bompard, I. Amat, X. Fauvergue, T. Spataro, Host-Parasitoid Dynamics and the Success of Biological Control When Parasitoids Are Prone to Allee Effects, *PLoS One*, **8** (2013), e76768. https://doi.org/10.1371/journal.pone.0076768
16. Y. Kuang, *Delay Differential Equations: with Applications in Population Dynamics*, Academic Pres, Boston, 1993. https://doi.org/10.1016/0378-4754(93)90045-V
17. A. Martin, S. Ruan, Predator-prey models with delay and prey harvesting, *J. Math. Biol.*, **43** (2001), 247–267. https://doi.org/10.1007/s002850100095

18. J. Xia, Z. Liu, R. Yuan, S. Ruan, The effects of harvesting and time delay on predator-prey systems with Holling type II functional response, *SIAM J. Appl. Math.*, **70** (2009), 1178–1200. https://api.semanticscholar.org/CorpusID:6516128
19. Q. An, W. Jiang, Spatiotemporal attractors generated by the Turing-Hopf bifurcation in a time-delayed reaction-diffusion system, *Discrete Cont. Dyn. B*, **24** (2019), 487–510. https://doi.org/10.3934/DCDSB.2018183
20. Y. Song, T. Zhang, Y. Peng, Turing-Hopf bifurcation in the reaction-diffusion equations and its applications, *Commun. Nonlinear Sci.*, **33** (2016), 229–258. https://doi.org/10.1016/j.cnsns.2015.10.002
21. Y. Song, H. Jiang, Y. Yuan, Turing-Hopf bifurcation in the reaction-diffusion equations and its applications, *J. Appl. Anal. Comput.*, **9** (2019), 1132–1164. https://doi.org/10.11948/2156-907X.20190015
22. B. Dai, G. Sun, Turing-Hopf bifurcation of a delayed diffusive predator-prey system with chemotaxis and fear effect, *Appl. Math. Lett.*, **111** (2021), 106644. https://doi.org/10.1016/j.aml.2020.106644
23. W. Jiang, Q. An, J. Shi, Formulation of the normal form of Turing-Hopf bifurcation in partial functional differential equations, *J. Differ. Equation*, **268** (2020), 6067–6102. https://doi.org/10.1016/j.jde.2019.11.039
24. J. Wang, J. Wei, J. Shi, Global bifurcation analysis and pattern formation in homogeneous diffusive predator-prey systems, *J. Differ. Equation*, **260** (2016), 3495–3523. https://doi.org/10.1016/j.jde.2015.10.036
25. X. Wang, Y. Cai, H. Ma, Dynamics of a diffusive predator-prey model with Allee effect on predator, *Discrete Dyn. Nat. Soc.*, **2013** (2013), 1–10. https://doi.org/10.1155/2013/984960
26. Y. V. Tyutyunov, D. Sen, L. I. Titova, M. Banerjee, Predator overcomes the Allee effect due to indirect prey-taxis, *Ecol. Complex.*, **39** (2019), 10772. https://doi.org/10.1016/j.ecocom.2019.100772
27. S. Rana, A. R. Bhowmick, T. Sardar, Invasive dynamics for a predator-prey system with Allee effect in both populations and a special emphasis on predator mortality, *Chaos*, **31** (2021), 033150. https://doi.org/10.1063/5.0035566
28. J. Guckenheimer, P. Holmes, *Nonlinear oscillations, dynamical systems, and bifurcations of vector fields*, 1^{st} edition, Springer-Verlag, New York, 1983. https://doi.org/10.1007/978-1-4612-1140-2
29. R. J. LeVeque, *Finite difference methods for ordinary and partial differential equations: steady-state and time-dependent problems*, 1^{st} edition, Society for Industrial and Applied Mathematics, Philadelphia, 2007. https://doi.org/10.1137/1.9780898717839
30. D. Ghosh, P. K. Santra, G. S. Mahapatra, A three-component prey-predator system with interval number, *Math. Model. Numer. Simul. Appl.*, **3** (2023), 1–16. https://api.semanticscholar.org/CorpusID:258151606
31. P. A. Naik, Z. Eskandari, H. E. Shahraki, Flip and generalized flip bifurcations of a two-dimensional discrete-time chemical model, *Math. Model. Numer. Simul. Appl.*, **1** (2021), 95–101. https://doi.org/10.53391/mmnsa.2021.01.009

32. P. A. Naik, Z. Eskandari, M. Yavuz, J. Zu, Complex dynamics of a discrete-time Bazykin Berezovskaya prey-predator model with a strong Allee effect, *J. Comput. Appl. Math.*, **413** (2022), 114401. https://doi.org/10.1016/j.cam.2022.114401

33. M. Manica, R. Rosa, A. Pugliese, L. Bolzoni, Exclusion and spatial segregation in the apparent competition between two hosts sharing macroparasites, *Theor. Popul. Biol.*, **86** (2013), 12–22. https://doi.org/10.1016/j.tpb.2013.03.002

34. L. D. Fernandes, M. A. Aguiar, Turing patterns and apparent competition in predator-prey food webs on networks, *Phys. Rev. E Stat. Nonlinear Soft Matter Phys.*, **86** (2012), 056203. https://doi.org/10.1103/PhysRevE.86.056203

35. H. Chen, C. Zhang, Bifurcations and hydra effects in a reaction-diffusion predator-prey model with Holling II functional response, *J. Appl. Anal. Comput.*, **13** (2023), 424–444. https://doi.org/10.11948/20220221

36. M. Yavuz, N. Sene, Stability analysis and numerical computation of the fractional predator-prey model with the harvesting rate, *Fractal Fract.*, **4** (2020), 35. https://doi.org/10.3390/fractalfract4030035

37. A. Chatterjee, S. Pal, A predator-prey model for the optimal control of fish harvesting through the imposition of a tax, *Int. J. Optim. Control, Theor. Appl.* , **13** (2023), 68–80. https://doi.org/10.11121/ijocta.2023.1218

Appendix: The coefficient of quadratic and cubic terms

The expressions of the coefficients in (3.7) are as follows.

$$
\begin{aligned}
f^{11}_{\alpha_1 z_1} =& 2\psi_1(0)\left[L_1\phi_1(0)+L_2\phi_1(-1)\right], \quad f^{11}_{\alpha_2 z_1}=0,\\
f^{13}_{\alpha_1 z_2} =& 2\psi_2(0)\left[-\frac{n_2^2}{l^2}D_1^{(1,0)}\phi_2(0)+L_1\phi_2(0)+L_2\phi_2(-1)\right], \quad f^{13}_{\alpha_2 z_2}=-2\psi_2(0)\frac{n_2^2}{l^2}D_1^{(0,1)}\phi_2(0),\\
g^{11}_{210} =& f^{11}_{210}+\frac{3}{2\mathrm{i}\omega_0\tau_*}\left(-f^{11}_{110}f^{11}_{200}+f^{11}_{110}f^{12}_{110}+\frac{2}{3}f^{11}_{020}f^{12}_{200}\right)+\frac{3}{2}\psi_1(0)\left[S_{yz_1}(\langle h_{110}(\theta)\beta_{n_1},\beta_{n_1}\rangle)\right.\\
&\left.+S_{y\bar{z}_1}(\langle h_{200}(\theta)\beta_{n_1},\beta_{n_1}\rangle)\right],\\
g^{11}_{102} =& f^{11}_{102}+\frac{3}{2\mathrm{i}\omega_0\tau_*}\left(-2f^{11}_{002}f^{11}_{200}+f^{12}_{002}f^{11}_{110}+2f^{11}_{002}f^{13}_{101}\right)+\frac{3}{2}\psi_1(0)\left[S_{yz_1}(\langle h_{002}(\theta)\beta_{n_1},\beta_{n_1}\rangle)\right.\\
&\left.+S_{yz_2}(\langle h_{101}(\theta)\beta_{n_2},\beta_{n_1}\rangle)\right],\\
g^{13}_{111} =& f^{13}_{111}+\frac{3}{2\mathrm{i}\omega_0\tau_*}\left(-f^{13}_{101}f^{11}_{110}+f^{13}_{011}f^{12}_{110}\right)+\frac{3}{2}\psi_2(0)\left[S_{yz_1}(\langle h_{011}(\theta)\beta_{n_1},\beta_{n_2}\rangle)+S_{y\bar{z}_1}(\langle h_{101}(\theta)\beta_{n_1},\beta_{n_2}\rangle)\right.\\
&\left.+S_{yz_2}(\langle h_{110}(\theta)\beta_{n_2},\beta_{n_2}\rangle)\right],\\
g^{13}_{003} =& f^{13}_{003}+\frac{3}{2\mathrm{i}\omega_0\tau_*}\left(-f^{11}_{002}f^{13}_{101}+f^{12}_{002}f^{13}_{011}\right)+\frac{3}{2}\psi_2(0)\left[S_{yz_2}(\langle h_{002}(\theta)\beta_{n_2},\beta_{n_2}\rangle)\right].
\end{aligned}
$$

Here $f_{mnk}^{12} = \overline{f_{mnk}^{11}}$,

$$
\begin{aligned}
&f_{mnk}^{11} = \frac{1}{\sqrt{l\pi}}\psi_1(0)F_{mnk}, \quad f_{mnk}^{13} = \frac{1}{\sqrt{l\pi}}\psi_2(0)F_{mnk}, \quad m+n+k=2,\\
&f_{210}^{11} = \frac{1}{l\pi}\psi_1(0)F_{210}, \quad f_{102}^{11} = \frac{1}{l\pi}\psi_1(0)F_{102}, \quad f_{111}^{13} = \frac{1}{l\pi}\psi_2(0)F_{111}, \quad f_{003}^{13} = \frac{3}{2l\pi}\psi_2(0)F_{003}.\\
&\langle h_{200}(\theta)\beta_{n_1},\beta_{n_1}\rangle = \frac{e^{2\mathrm{i}\omega_0\tau_*\theta}}{l\pi}\left[2\mathrm{i}\omega_0\tau_* - L_0\left(e^{2\mathrm{i}\omega_0\tau_*\cdot}I_d\right)\right]^{-1}F_{200} - \frac{1}{\mathrm{i}\omega_0\tau_*\sqrt{l\pi}}\left[f_{200}^{11}\phi_1(\theta) + \frac{1}{3}f_{200}^{12}\overline{\phi}_1(\theta)\right],\\
&\langle h_{110}(\theta)\beta_{n_1},\beta_{n_1}\rangle = -\frac{1}{l\pi}\left[L_0(I_d)\right]^{-1}F_{110} + \frac{1}{\mathrm{i}\omega_0\tau_*\sqrt{l\pi}}\left[f_{110}^{11}\phi_1(\theta) - f_{110}^{12}\overline{\phi}_1(\theta)\right],\\
&\langle h_{110}(\theta)\beta_{n_2},\beta_{n_2}\rangle = \langle h_{110}(\theta)\beta_{n_1},\beta_{n_1}\rangle,\\
&\langle h_{101}(\theta)\beta_{n_2},\beta_{n_1}\rangle = \frac{e^{\mathrm{i}\omega_0\tau_*\theta}}{l\pi}\left[\mathrm{i}\omega_0\tau_* + \frac{n_2^2}{l^2}D_0 - L_0\left(e^{\mathrm{i}\omega_0\tau_*\cdot}I_d\right)\right]^{-1}F_{101} - \frac{1}{\mathrm{i}\omega_0\tau_*\sqrt{l\pi}}f_{101}^{13}\phi_2(0),\\
&\langle h_{011}(\theta)\beta_{n_1},\beta_{n_2}\rangle = \frac{e^{-\mathrm{i}\omega_0\tau_*\theta}}{l\pi}\left[-\mathrm{i}\omega_0\tau_* + \frac{n_2^2}{l^2}D_0 - L_0\left(e^{-\mathrm{i}\omega_0\tau_*\cdot}I_d\right)\right]^{-1}F_{011} + \frac{1}{\mathrm{i}\omega_0\tau_*\sqrt{l\pi}}f_{011}^{13}\phi_2(0),\\
&\langle h_{002}(\theta)\beta_{n_1},\beta_{n_1}\rangle = -\frac{1}{l\pi}\left[L_0(I_d)\right]^{-1}F_{002} + \frac{1}{\mathrm{i}\omega_0\tau_*\sqrt{l\pi}}\left[f_{002}^{11}\phi_1(\theta) - f_{002}^{12}\overline{\phi}_1(\theta)\right],\\
&\langle h_{002}(\theta)\beta_{n_2},\beta_{n_2}\rangle = \frac{1}{2l\pi}\left[\frac{4n_2^2}{l^2}D_0 - L_0(I_d)\right]^{-1}F_{002} + \langle h_{002}(\theta)\beta_{n_1},\beta_{n_1}\rangle,
\end{aligned}
$$

with

$$
\begin{aligned}
F_{200} =& F_{uu} + 2k_1\left(F_{uv} + F_{vv_\tau}k_1e^{-\mathrm{i}\omega_0\tau_*} + F_{u_\tau v_\tau}e^{-2\mathrm{i}\omega_0\tau_*} + F_{u_\tau v}e^{-\mathrm{i}\omega_0\tau_*}\right) + F_{vv}k_1^2 + F_{u_\tau u_\tau}e^{-2\mathrm{i}\omega_0\tau_*},\\
F_{110} =& 2\Big[F_{uu} + F_{vv}k_1\overline{k}_1 + F_{u_\tau u_\tau} + F_{uv}\left(k_1+\overline{k}_1\right) + F_{u_\tau v}\left(\overline{k}_1e^{-\mathrm{i}\omega_0\tau_*} + k_1e^{\mathrm{i}\omega_0\tau_*}\right) + F_{vv_\tau}k_1\overline{k}_1\left(e^{-\mathrm{i}\omega_0\tau_*} + e^{\mathrm{i}\omega_0\tau_*}\right)\\
&+F_{u_\tau v_\tau}\left(k_1+\overline{k}_1\right)\Big],\\
F_{101} =& 2\Big[F_{uu} + F_{vv}k_1k_3 + F_{u_\tau u_\tau}e^{-\mathrm{i}\omega_0\tau_*} + F_{uv}\left(k_1+k_3\right) + F_{u_\tau v}\left(k_1 + k_3e^{-\mathrm{i}\omega_0\tau_*}\right) + F_{vv_\tau}k_1k_3\left(1+e^{-\mathrm{i}\omega_0\tau_*}\right)\\
&+F_{u_\tau v_\tau}\left(k_1+k_3\right)e^{-\mathrm{i}\omega_0\tau_*}\Big],\\
F_{002} =& F_{uu} + F_{vv}k_3^2 + F_{u_\tau u_\tau} + 2\left(F_{uv}k_3 + F_{u_\tau v}k_3 + F_{vv_\tau}k_3^2 + F_{u_\tau v_\tau}k_3\right),\\
F_{002} =& \overline{F_{200}}, \quad F_{011} = \overline{F_{101}},\\
F_{210} =& 3\Big[F_{uuu} + F_{uuv}\left(2k_1+\overline{k}_1\right) + F_{vvv}k_1^2\overline{k}_1 + F_{u_\tau vv}k_1\left(2\overline{k}_1e^{-\mathrm{i}\omega_0\tau_*} + k_1e^{\mathrm{i}\omega_0\tau_*}\right) + F_{vvv_\tau}k_1^2\overline{k}_1\left(2e^{-\mathrm{i}\omega_0\tau_*} + e^{\mathrm{i}\omega_0\tau_*}\right)\\
&+F_{u_\tau u_\tau v}\left(2k_1 + \overline{k}_1e^{-2\mathrm{i}\omega_0\tau_*}\right) + 2F_{u_\tau vv_\tau}k_1\left(\overline{k}_1 + \overline{k}_1e^{-2\mathrm{i}\omega_0\tau_*} + k_1\right) + F_{u_\tau u_\tau v_\tau}\left(2k_1e^{-\mathrm{i}\omega_0\tau_*} + \overline{k}_1e^{-\mathrm{i}\omega_0\tau_*}\right)\\
&+F_{u_\tau u_\tau u_\tau}e^{-\mathrm{i}\omega_0\tau_*}\Big],\\
F_{102} =& 3\Big[F_{uuu} + F_{uuv}\left(k_1+2k_3\right) + F_{vvv}k_1k_3^2 + F_{u_\tau vv}k_3\left(k_3e^{-\mathrm{i}\omega_0\tau_*} + 2k_1\right) + F_{vvv_\tau}k_1k_3^2\left(2+e^{-\mathrm{i}\omega_0\tau_*}\right)\\
&+F_{u_\tau u_\tau v}\left(k_1 + 2k_3e^{-\mathrm{i}\omega_0\tau_*}\right) + 2F_{u_\tau vv_\tau}k_3\left(k_1 + k_3e^{-\mathrm{i}\omega_0\tau_*} + k_1e^{-\mathrm{i}\omega_0\tau_*}\right) + F_{u_\tau u_\tau v_\tau}\left(k_1e^{-\mathrm{i}\omega_0\tau_*} + 2k_3e^{-\mathrm{i}\omega_0\tau_*}\right)\\
&+F_{u_\tau u_\tau u_\tau}e^{-\mathrm{i}\omega_0\tau_*}\Big],
\end{aligned}
$$

$$
\begin{aligned}
F_{111} =& 6\Big\{F_{uuv}\left(k_1+k_3+\bar{k}_1\right)+F_{u_\tau vv}\left(k_1\bar{k}_1+\bar{k}_1k_3e^{-\mathrm{i}\omega_0\tau_*}+k_1k_3e^{\mathrm{i}\omega_0\tau_*}\right)+F_{vvv_\tau}k_1\bar{k}_1k_3\left(1+e^{-\mathrm{i}\omega_0\tau_*}+e^{\mathrm{i}\omega_0\tau_*}\right)\\
&+F_{u_\tau u_\tau v}\left(k_3+k_1e^{\mathrm{i}\omega_0\tau_*}+e^{-\mathrm{i}\omega_0\tau_*}\bar{k}_1\right)+F_{uuu}+F_{u_\tau u_\tau u_\tau}+F_{u_\tau u_\tau v_\tau}\left(k_1+k_3+\bar{k}_1\right)+F_{vvv}k_1\bar{k}_1k_3\\
&+F_{u_\tau vv_\tau}\left[k_1k_3\left(1+e^{\mathrm{i}\omega_0\tau_*}\right)+k_1\bar{k}_1\left(e^{-\mathrm{i}\omega_0\tau_*}+e^{\mathrm{i}\omega_0\tau_*}\right)+\bar{k}_1k_3\left(1+e^{-\mathrm{i}\omega_0\tau_*}\right)\right]\Big\},\\
F_{003} =& F_{uuu}+F_{vvv}k_3^3+F_{u_\tau u_\tau u_\tau}+3k_3\left(F_{uuv}+F_{u_\tau u_\tau v_\tau}+F_{u_\tau u_\tau v}+F_{u_\tau vv}k_3+2F_{u_\tau vv_\tau}k_3+F_{vvv_\tau}k_3^2\right),
\end{aligned}
$$

and the linear operators $S_{yz_i}(i=1,2)$ from Q^1 to $X_{\mathbb{C}}$ are defined as follow:

$$
\begin{aligned}
S_{yz_i}(\varphi) &= \left(F_{y_1(0)z_i},F_{y_2(0)z_i}\right)\varphi(0)+\left(F_{y_1(-1)z_i},F_{y_2(-1)z_i}\right)\varphi(-1),\\
S_{y\bar{z}_1}(\varphi) &= \left(\overline{F_{y_1(0)z_1}},\overline{F_{y_2(0)z_1}}\right)\varphi(0)+\left(\overline{F_{y_1(-1)z_1}},\overline{F_{y_2(-1)z_1}}\right)\varphi(-1),
\end{aligned}
$$

where

$$
\begin{aligned}
F_{y_1(0)z_1} &= 2\left(F_{uu}+F_{uv}k_1\right), & F_{y_2(0)z_1} &= 2\left(F_{uv}+F_{vv}k_1+F_{u_\tau v}e^{-\mathrm{i}\omega_0\tau^*}+F_{vv_\tau}k_1e^{-\mathrm{i}\omega_0\tau_*}\right),\\
F_{y_2(-1)z_1} &= 2\left(F_{vv_\tau}k_1+F_{u_\tau v_\tau}e^{-\mathrm{i}\omega_0\tau^*}\right), & F_{y_1(-1)z_1} &= 2\left(F_{u_\tau v}k_1+F_{u_\tau u_\tau}e^{-\mathrm{i}\omega_0\tau_*}+F_{u_\tau v_\tau}k_1e^{-\mathrm{i}\omega_0\tau_*}\right),\\
F_{y_1(0)z_2} &= 2\left(F_{uu}+F_{uv}k_3\right), & F_{y_1(-1)z_2} &= 2\left(F_{u_\tau v}k_3+F_{u_\tau u_\tau}+F_{u_\tau v_\tau}k_3\right),\\
F_{y_2(0)z_2} &= 2\left(F_{uv}+F_{vv}k_3+F_{u_\tau v}+F_{vv_\tau}k_3\right), & F_{y_2(-1)z_2} &= 2\left(F_{vv_\tau}k_3+F_{u_\tau v_\tau}\right).
\end{aligned}
$$

The above expressions still needs the second and third derivatives of $\mathcal{F}(\alpha,U^t)$ with respect to $u(t)$, $v(t)$, $u(t-1)$, $v(t-1)$ at $(\alpha,U^t)=(0,0)$. Denote by $u(t)$, $v(t)$, $u(t-1)$, $v(t-1)$ the simplified form of u, v, u_τ, v_τ, respectively. Through direct calculation, one can see that the nonzero partial derivatives are

$$
\begin{aligned}
&F_{uu}=\begin{pmatrix}a_1\tau_*\\0\end{pmatrix}, \quad F_{uv}=\begin{pmatrix}a_2\tau_*\\0\end{pmatrix}, \quad F_{u_\tau u_\tau}=\begin{pmatrix}0\\b_1\tau_*\end{pmatrix}, \quad F_{u_\tau v}=\begin{pmatrix}0\\b_2\tau_*\end{pmatrix},\\
&F_{u_\tau v_\tau}=\begin{pmatrix}0\\b_3\tau_*\end{pmatrix}, \quad F_{vv}=\begin{pmatrix}0\\b_4\tau_*\end{pmatrix}, \quad F_{vv_\tau}=\begin{pmatrix}0\\b_5\tau_*\end{pmatrix}, \quad F_{uuu}=\begin{pmatrix}a_3\tau_*\\0\end{pmatrix},\\
&F_{uuv}=\begin{pmatrix}a_4\tau^*\\0\end{pmatrix}, \quad F_{u_\tau u_\tau u_\tau}=\begin{pmatrix}0\\b_6\tau_*\end{pmatrix}, \quad F_{u_\tau u_\tau v}=\begin{pmatrix}0\\b_7\tau_*\end{pmatrix}, \quad F_{u_\tau u_\tau v_\tau}=\begin{pmatrix}0\\b_8\tau_*\end{pmatrix},\\
&F_{u_\tau vv}=\begin{pmatrix}0\\b_9\tau_*\end{pmatrix}, \quad F_{u_\tau vv_\tau}=\begin{pmatrix}0\\b_{10}\tau_*\end{pmatrix}, \quad F_{vvv}=\begin{pmatrix}0\\b_{11}\tau_*\end{pmatrix}, \quad F_{vvv_\tau}=\begin{pmatrix}0\\b_{12}\tau_*\end{pmatrix},
\end{aligned}
$$

where a_i, b_j $(i=1,\cdots,4,\ j=1,2,\cdots,12)$ are defined in (3.2).